Corynebacterium Comparative Genomics Reveals a Role for Cobamide Sharing in the Skin Microbiome

Mary Hannah Swaney[1] and Lindsay R Kalan[1,2]

[1]Department of Medical Microbiology and Immunology, School of Medicine and Public Health, University of Wisconsin, Madison, WI, USA

[2]Department of Medicine, School of Medicine and Public Health, University of Wisconsin, Madison, WI, USA

Address for Correspondence: Lindsay R. Kalan, 1550 Linden Dr, 6155 Microbial Sciences Building, Madison, WI, USA, 53706. lkalan@wisc.edu

ABSTRACT

The human skin microbiome is a key player in human health, with diverse functions ranging from defense against pathogens to education of the immune system. Recent studies have begun unraveling the complex interactions within skin microbial communities, shedding light on the invaluable role that skin microorganisms have in maintaining a healthy skin barrier. While the *Corynebacterium* genus is a dominant taxon of the skin microbiome, relatively little is known how skin-associated Corynebacteria contribute to microbe-microbe and microbe-host interactions on the skin. Here, we performed a comparative genomics analysis of 71 *Corynebacterium* species from diverse ecosystems, which revealed functional differences between host- and environment-associated species. In particular, host-associated species were enriched for *de novo* biosynthesis of cobamides, which are a class of cofactor essential for metabolism in organisms across the tree of life but are produced by a limited number of prokaryotes. Because cobamides have been hypothesized to mediate community dynamics within microbial communities, we analyzed skin metagenomes for *Corynebacterium* cobamide producers, which revealed a positive correlation between cobamide producer abundance and microbiome diversity, a trait associated with skin health. We also provide the first metagenome-based assessment of cobamide biosynthesis and utilization in the skin microbiome, showing that both dominant and low abundant skin taxa encode for the *de novo* biosynthesis pathway and that cobamide-dependent enzymes are encoded by phylogenetically diverse taxa across the major bacterial phyla on the skin. Taken together, our results support a role for cobamide sharing within skin microbial communities, which we hypothesize mediates community dynamics.

INTRODUCTION

The human skin supports a diverse and complex ecosystem of bacterial, fungal, viral, and microeukaryote species, termed the skin microbiome. Highly adapted to live on the skin, these microorganisms form distinct and specialized communities across the various microenvironments of the skin, which include sebaceous, moist, dry, and foot sites. Rather than existing as innocuous bystanders, the skin microbiome plays a significant role in human health through contributing to immune system education and homeostasis, protecting against pathogen colonization, and promoting barrier maintenance and repair [1–6].

Advances in sequencing technology have allowed us to not only identify the taxa that comprise the microbial communities of the skin, but also to ascertain the functional potential of the skin microbiome and the contribution of particular taxa to microbiome structure, stability, and function. For example, genomics-guided approaches have identified a *Cutibacterium acnes* biosynthetic gene cluster that produces the novel small-molecule cutimycin, contributing to niche competition within the hair follicle microbial community [7]. In addition, pangenomic analyses of dominant skin species have revealed the potential for functional niche saturation in the skin microbiome, where distinct combinations of strains within the same species contribute similar genetic potential [8]. Genomics studies have also elucidated the lineage-specific genetic differences between *C. acnes* strains that may explain the dual commensal and pathogenic phenotypes exhibited by this skin species [9]. These studies exemplify the power of sequence data analysis in generating hypotheses and gathering functional insight to skin microbial communities.

The transition from taxonomic characterization of the skin microbiome towards the elucidation of microbe-microbe and microbe-host interactions has shed light on the truly complex nature of skin microbial communities. Recent work has demonstrated that skin commensals not only take part in synergistic and competitive interactions within skin microbial communities [10–13], but also participate in microbe-host interactions that can dictate skin health and community structure [1,14–16]. While these studies have provided fundamental insight into the roles that certain skin commensals, particularly *Staphylococcus* species and *C. acnes*, play on the skin, little is known regarding the contribution of other major taxa residing within the skin.

Until recently, species of the *Corynebacterium* genus have been underappreciated as significant members of skin microbial communities, predominantly due to the difficulty of growing these species in the lab, which is a result of their nutritionally fastidious and slow-growing nature [17].

However, sequencing efforts have revealed that Corynebacteria are a dominant taxon within the microbiome, particularly in moist skin microenvironments [8,18,19]. Further, recent studies have exemplified the importance of certain *Corynebacterium* species in limiting pathogen colonization and virulence [20,21] and modulating the host response [22,23]. Considering the prevalence and diversity of commensal *Corynebacterium* species on the skin, their full potential in mediating interactions within the microbiome is likely much more vast.

To identify functions important for skin colonization by commensal *Corynebacterium* species, we performed a comparative genomics analysis of 71 species from the *Corynebacterium* genus, including species from a diverse host and environment niche range, and have generated the most up-to-date phylogeny of the *Corynebacterium* genus. Our analysis revealed that a subset of skin-associated *Corynebacterium* species encode for *de novo* biosynthesis of cobamides, a class of cofactor that is essential for metabolism in many organisms across life but only produced by a small fraction of prokaryotes. Microbiome diversity analysis of taxonomic data from 585 published skin metagenomes revealed that the abundance of cobamide-producing *Corynebacterium* species is associated with higher microbiome diversity, suggesting a role for cobamides in mediating skin microbiome community dynamics. We then analyzed 906 publicly available skin metagenomes to predict cobamide dependence and biosynthesis within the skin microbiome and found that phylogenetically diverse skin taxa are likely to use cobamides. Taken together, our results suggest that cobamide sharing occurs within the skin microbiome and hypothesize that this is an area of importance in studying community dynamics.

METHODS

Corynebacterium comparative genomics

71 *Corynebacterium* isolate genomes were acquired either from the National Center for Biotechnology Information (NCBI) as complete assemblies or from human skin isolates as draft assemblies. Supplementary Material S1 reports accession numbers and other information for each isolate genome, including ecosystem association, which was assigned using genome metadata and species-specific literature. The pangenomics workflow from anvi'o v6.2 (http://merenlab.org/2016/11/08/pangenomics-v2/) [24,25] was used for comparative genomics analysis. Briefly, genomes were annotated using 'anvi-run-ncbi-cogs', which assigns functions from the Clusters of Orthologous Groups (COGs) database. The *Corynebacterium* pangenome was computed using the program 'anvi-pan-genome' was used with the flags '--minbit 0.5', --mcl-inflation 6', and '--enforce-hierarchical-clustering'. Average nucleotide identity between genomes

129 was calculated using pyani within the anvi'o environment (https://github.com/widdowquinn/pyani)
130 [26]. The program 'anvi-get-enriched-functions-per-pan-group' was utilized to identify enriched
131 COGs between host- and environment-associated genomes. Genome summary statistics are
132 presented in Table S1.
133
134 ***Corynebacterium* phylogenetic analysis**
135 The anvi'o phylogenomics workflow (http://merenlab.org/2017/06/07/phylogenomics/) was used
136 to create a *Corynebacterium* phylogeny. Within the anvi'o environment, single copy genes (SCGs)
137 from the curated anvi'o collection Bacteria_71 were identified within each genome using
138 hmmscan from the HMMER package (http://hmmer.org/), and the SCG amino acid sequences
139 were concatenated and aligned using MUSCLE [27]. A phylogenomic tree was constructed using
140 FastTree [28] within anvi'o. To identify cobamide biosynthesis genes within the 71
141 *Corynebacterium* genomes, 46 KEGG orthology (KO) identifiers from KEGG map00860
142 (porphyrin and chlorophyll metabolism) were used to create a custom profile for KOfamscan, a
143 functional annotation program based on KO and HMMs [29]. Each genome was queried against
144 this profile, and hits to the KOs above the predefined KOfamscan threshold were considered for
145 further analysis. Visualization of the phylogenomic tree and cobamide biosynthesis pathway
146 completeness was performed in R with the ggtree package [30].
147
148 **Microbiome diversity analysis of *Corynebacterium* cobamide producers**
149 Using the taxonomic abundance information from 585 skin metagenomes from Oh *et al*. [8], the
150 total sum abundance of 5 *Corynebacterium* species (*C. amycolatum, C. kroppenstedtii, C.*
151 *ulcerans, C. pseudotuberculosis, C. diphtheriae*) shown to encode for *de novo* cobamide
152 biosynthesis was calculated for each metagenome. Richness was determined by calculating the
153 total number of observed species within each sample. Alpha diversity was determined by
154 calculating the Shannon index using the diversity() function from the phyloseq v1.26.1 package
155 in R. The Spearman correlation between *Corynebacterium* cobamide producer abundance and
156 alpha diversity was calculated and plotted with ggscatter() and stat_cor() from the ggpubr v0.4.0
157 package. For beta diversity analysis, relative abundances were square root transformed to give
158 more weight to low abundance taxa, and the Bray-Curtis dissimilarity index was calculated for
159 samples within each skin site using vegdist() from the vegan v2.5-6 package. The indices were
160 ordinated using non-metric multidimensional scaling with the vegan metaMDS() program.
161
162 **Choice of profile HMMs for skin metagenome survey of cobamide biosynthesis and use**

Profile HMMs, retrieved from the TIGRfam and Pfam databases, were used to detect cobamide biosynthesis, cobamide transport, and cobamide-dependent genes within skin metagenomic sequencing data. A total of 12 cobamide biosynthesis genes were selected because of their broad distribution throughout both the aerobic and anaerobic biosynthesis pathways and their presence within taxonomically-diverse cobamide producer genomes [31–33]. CbiZ was included as a marker of cobamide remodeling, and BtuB was included to assess cobamide transport. 19 cobamide-dependent enzymes and proteins with B_{12}-binding domains were chosen to evaluate cobamide use. The single copy gene rpoB was used as a phylogenetic marker to assess microbial community structure within each metagenome and as a proxy for sequence depth. All cobamide-associated genes used in this analysis can be found in Supplementary Material S3.

Metagenomic sequence search using HMMER

Raw sequencing data from 906 skin metagenomes was retrieved from the Sequence Read Archive (SRA) and converted to FASTA format, retaining only forward read files for analysis (Supplemental Table S2). Metagenomes were translated to each of 6 frame translations using transeq from the emboss v6.6.0 package [34]. The program hmmsearch from HMMER v3.3.1 [35] was used with default parameters and an E-value cutoff of 1E-06 to scan the metagenomic sequencing reads for homology to each cobamide-related HMM. The resulting hits were taxonomically classified to the family, genus, and species levels using Kraken 2 [36] and Bracken [37]. The number of hits for each gene was normalized to HMM length when analyzing individual metagenomes and to both HMM length and sequencing depth when analyzing groups of metagenomes. Taxonomic frequency profiles were generated for each cobamide-related gene by dividing the normalized number of gene hits per taxon by the total normalized number of gene hits.

Metagenomic sequence search using INFERNAL

Covariance models (CMs) for 3 cobalamin riboswitches from the Rfam clan CL00101 were retrieved from the Rfam database [38] (Supplementary Material S4). The program cmsearch from INFERNAL v1.1.2 [39] was used with default parameters and an E-value cutoff of 1E-06 to scan the metagenomes for RNA homologs to cobalamin riboswitches. The methods following hit identification are the same as described above for HMM analysis, except that the number of hits for each riboswitch were not normalized by CM length because the read lengths and CM lengths were relatively similar.

197 **Mapping of cobalamin riboswitch hits to genomes**
198 Reads identified from INFERNAL were aligned against the genomes of *Cutibacterium acnes*
199 KPA171202, *Veillonella parvula* DSM 2008, *Corynebacterium* sp. ATCC 6931, *Pseudomonas*
200 *putida* KT2440, and *Streptococcus sanguinis* SK36 using bowtie2 v2.3.5.1 and visualized in R
201 with the ggbio v1.30.0 package. Genes upstream and downstream of the aligned reads within
202 each genome were assigned functions based on NCBI RefSeq annotations and visualized using
203 the gggenes v0.4.0 R package. Genes within genomic regions that encoded for a cobalamin
204 riboswitch but had no genes currently known to be under cobalamin riboswitch control were
205 assigned putative functions based on NCBI BLAST search results.
206
207 **RESULTS**
208
209 **Ecosystem association drives *Corynebacterium* genetic diversity.**
210 Species within the *Corynebacterium* genus occupy highly diverse habitats, including soil, cheese
211 rinds, coral mucus, and human skin, with certain species causing serious disease in humans and
212 animals. To explore the genomic diversity within the *Corynebacterium* genus, we performed a
213 pangenomic analysis using anvi'o. These analyses included 50 host-associated (HA) and 21
214 environment-associated (EA) genomes (Supplemental Table S1), acquired as complete
215 assemblies from NCBI (n=68) or as draft assemblies from human skin strains we isolated (n=3).
216 Gene clusters (GCs), which represent one or more genes contributed by one or more genomes,
217 were inferred using the anvi'o anvi-pan-genome function. Across all species, we identified 42,154
218 total GCs, 495 of which are core GCs present in all genomes. In a subset of genomes, 13,235
219 GCs are shared (dispensable) and 28,424 GCs are found in only one genome (species-specific)
220 (Figure 1). Genome size ranged from 2.0 to 3.6 Mbp, with an average of 2.7 ± 0.3 Mbp, and the
221 number of GCs per genome ranged from 1858 to 3170 GCs, with an average of 2365 ± 294 GCs
222 (Supplemental Table S1). Further, HA species have a significantly reduced average number of
223 GCs per genome compared to EA species (2242 vs. 2661, p-value<0.0001) and a significantly
224 reduced genome length (2.6 Mbp vs 3.0 Mbp, p-value<0.0001) (Figure 2A, 2B).
225
226 Because we observed significant differences in gene cluster number and genome size between
227 HA and EA genomes, we hypothesized that HA and EA *Corynebacterium* species would form
228 phylogenetically distinct clades. To test this hypothesis, we generated a *Corynebacterium*
229 phylogenetic tree based on 71 conserved single copy genes. We found that generally, EA and
230 HA species were interspersed throughout the phylogeny, with a few clear HA- or EA-specific

231 subgroups (Figure 3). For example, the HA *C. amycolatum* subgroup forms the deepest subline
232 within this genus, consistent with previous findings [40]. Species within this subgroup are unique
233 compared to most other Corynebacteria in that they do not contain mycolic acids in their cell walls.
234 In addition, the clade containing *C. diphtheriae* and *C. pseudotuberculosis* also consists uniquely
235 of HA species, several of which are serious pathogens in humans and other animals.
236 Furthermore, a distinct lineage of EA soil dwelling Corynebacteria is formed by several species
237 including *C. glutamicum,* which is an industrial producer of amino acids and other diverse
238 products. We also observed that genome length was reflected by the phylogeny, where species
239 within the same clade possessed similar genome length and EA clades having notably larger
240 genomes (Figure 3).
241
242 ***De novo* cobamide biosynthesis is enriched in host-associated Corynebacteria.**
243 To identify functional gene predictions that differ between HA and EA genomes, we performed a
244 functional enrichment analysis in anvi'o using Clusters of Orthologous Groups (COG) annotations.
245 Within the top significantly enriched functions in EA genomes, we observed functions putatively
246 involved in amino acid transport, metabolism of various substrates, including aromatic
247 compounds, tetrahydropterin cofactors, citrate/malate, and alcohols, and other uncharacterized
248 functions ($q < 0.05$) (Figure 2D). Within HA genomes, we observed a significant enrichment of
249 functions involved in the transport of various substrates, as well as 8 COG functions putatively
250 involved in cobamide biosynthesis in HA genomes ($q < 0.05$) (Fig. 2C). Cobamides, which consist
251 of the vitamin B_{12} family of cofactors, are required for metabolism by organisms across all domains
252 of life. Specifically, they function in the catalysis of diverse enzymatic reactions, ranging from
253 primary and secondary metabolism, including methionine and natural product synthesis, to
254 environmentally impactful processes, such as methanogenesis and mercury methylation.
255
256 To validate the presence of the enriched cobamide biosynthesis genes and other genes of the
257 approximately 25-enzyme cobamide biosynthesis pathway within the 71 *Corynebacterium*
258 genomes, we scanned the genomes for these genes using KOfamScan [29]. We found that
259 tetrapyrrole precursor synthesis, which is shared among the cobamide, heme, and chlorophyll
260 biosynthesis pathways [31], was highly conserved throughout the genus (Figure 3). Corrin ring
261 and nucleotide loop synthesis was predominantly intact and conserved within 5 distinct
262 *Corynebacterium* lineages, including those of *C. diphtheriae, C. epidermidicans, C.*
263 *argentoratense, C. kroppenstedtii,* and *C. amycolatum*. The species within these groups encode
264 for all or nearly all of the genes required for cobamide biosynthesis, and notably, 21 out of 22 of

265 these predicted cobamide producers are host-associated (Figure 3). In addition, three EA species
266 encode for the later portion of the pathway involved in nucleotide loop assembly, which can
267 function in cobinamide salvaging. Taken together, these observations demonstrate a range of
268 cobamide biosynthetic capabilities by Corynebacteria, including *de novo* producers, cobinamide
269 salvagers, and non-producers.
270
271 **Microbiome diversity is associated with the abundance of *Corynebacterium* cobamide**
272 **producers.** While 86% of bacteria have been found to encode at least one cobamide-dependent
273 enzyme, only 37% of bacteria can produce the cofactor *de novo* [31]. Therefore, within microbial
274 communities, cobamide sharing likely exists as a means to fulfill this nutritional requirement and
275 is hypothesized to mediate community dynamics. Because several skin-associated
276 Corynebacteria were identified to encode for *de novo* cobamide biosynthesis, we hypothesize
277 that cobamide sharing occurs in the skin microbiome and mediates community dynamics. To
278 assess changes at the community level associated with the presence of *Corynebacterium*
279 cobamide producers, we explored the relationship between microbiome diversity and the
280 abundance of Corynebacterium species producing cobamides. To do this, we analyzed published
281 relative abundance data from 585 skin metagenomes [8]. Within each metagenome, we summed
282 the abundance of five *Corynebacterium* species that encode for *de novo* cobamide biosynthesis
283 (*C. amycolatum, C. kroppenstedtii, C. diphtheriae, C. ulcerans, C. tuberculosis*) and analyzed
284 diversity within each community. We found that the abundance of these cobamide producers was
285 positively correlated with alpha diversity (Shannon index) in 12/18 skin sites ($p<0.05$) (Figure 4A),
286 suggesting that increased abundance of cobamide-producing Corynebacteria (CPC) within the
287 community may increase diversity. We also observed a positive correlation between CPC
288 abundance and community richness, although only in 4/18 skin sites ($p<0.05$) (Supplemental
289 Figure 1). The observation that CPC abundance overall has a higher correlation with Shannon
290 diversity, a metric taking into account total number of species and their overall proportion,
291 compared to total species counts suggests that the increase in diversity we observe arises
292 predominantly from an increase in species evenness within a given community. Supporting this
293 argument, we found that communities with a low CPC abundance were usually dominated by
294 single species including *Cutibacterium acnes* (formerly *Propionibacterium acnes*) and
295 *Propionibacterium* phage, while communities with high CPC showed an expansion of other skin
296 taxa and an overall more even species distribution within the community (Supplemental Figure
297 2).
298

299 To determine if CPC also shapes community composition, we calculated the Bray-Curtis
300 dissimilarity index of square-root transformed abundance data of all samples within each skin site.
301 A square root transformation was applied in order to give less weight to dominant species and
302 more weight to low abundant species, which were prevalent in the dataset. The resulting matrices
303 were ordinated by non-metric multidimensional scaling to visualize relatedness between
304 individual communities. Within skin sites, particularly those that demonstrated a positive
305 correlation between Shannon diversity and CPC abundance, samples clustered along gradients
306 of both alpha diversity and CPC abundance (Figure 4B). This was especially evident for samples
307 in the alar crease, back, manubrium, and inguinal crease, each of which had the strongest
308 correlation coefficients between Shannon diversity and CPC abundance (R=0.82, R=0.87,
309 R=0.67, R=0.79 respectively) (Figure 4A).
310
311 **Cobamide biosynthesis, salvage, and remodeling genes are encoded by skin taxa.**
312 Having identified that several skin-associated *Corynebacterium* species encode for *de novo*
313 cobamide biosynthesis, we were interested in determining if other members within the skin
314 microbiome also had this genomic capacity. We searched for cobamide biosynthesis genes within
315 906 skin metagenomes, encompassing samples from 21 distinct skin sites of 2 independent skin
316 microbiome surveys [8,78] (Supplemental Table S2). We used 12 profile HMMs representing
317 genes that demonstrated broad distribution within the *de novo* cobamide biosynthesis pathway
318 and have been previously used to identify cobamide biosynthesis genes within metagenomic data
319 [32,33]. Among site microenvironments, sebaceous sites were revealed to harbor the overall
320 highest number of hits to cobamide biosynthesis genes (n=139,128 reads), followed by moist
321 sites (n=36,845 reads), dry sites (n=31,645 reads), and foot sites (n=6,411 reads) (Supplemental
322 Material S5). To assess the contribution of different taxa to cobamide biosynthesis, the
323 metagenomic sequence classifier pipeline Kraken and Bracken was used to taxonomically
324 classify the resulting gene hits. We identified the top taxa encoding for biosynthetic genes in
325 descending order to be Propionibacteriaceae (n=190,437 reads), Pseudomonadaceae (n=4,248
326 reads), Corynebacteriaceae (n=3,274 reads), Veillonellaceae (n=2036 reads), and
327 Streptococcaceae (n=1,337 reads) (Supplemental Material S6). Within individual metagenomes,
328 we calculated the contribution of each taxa to cobamide biosynthesis gene hits by dividing the
329 number of gene hits assigned to a given taxa by the total number of gene hits within the sample.
330 We found that Propionibacteriaceae was the dominant contributor to cobamide biosynthesis gene
331 hits, particularly in sebaceous sites (Figure 5). However, metagenomes from moist, dry, and foot

332 sites exhibited higher variability in Propionibacteriaceae contribution, which was also reflected in
333 variable contribution by the other four taxa.
334
335 For a finer resolution of taxa contribution across individual biosynthesis genes, we determined
336 taxa contribution to 12 cobamide biosynthesis marker genes for the top 40 abundant taxa within
337 the dataset. This analysis revealed that the number of taxa encoding the full or nearly complete
338 suite of cobamide biosynthesis markers varied according to the microenvironment (Figure 6). In
339 particular, cobamide biosynthetic potential within the sebaceous microenvironment is uniquely
340 restricted to Propionibacteriaceae, whereas numerous taxa within the moist, dry, and foot
341 microenvironments encode for most cobamide biosynthesis markers. These include diverse taxa
342 across the Firmicutes, Actinobacteria, and Proteobacteria phyla, such as Pseudomonadaceae,
343 Veillonellaceae, and Rhodobacteraceae, all of which have previously been implicated in
344 cobamide biosynthesis [41–43]. Corynebacteriaceae were also found to encode for nearly all
345 cobamide biosynthesis markers, validating our comparative genomics analysis that identified
346 specific *Corynebacterium* species as *de novo* producers. We also observed that a proportion of
347 low abundant skin taxa encode for the full suite of cobamide biosynthesis markers, grouped into
348 the "Other" category (<0.15% abundance based on rpoB hits), demonstrating that cobamide
349 biosynthesis is likely encoded by low abundant or rare taxa as well. Overall, our analysis suggests
350 the dominant cobamide producers on the skin are Propionibacteriaceae and Corynebacteriaceae,
351 with other low abundant or rare taxa such as Veillonellaceae and Pseudomonodaceae
352 contributing to biosynthesis in a site dependent manner [8].
353
354 Furthermore, certain taxa such as Moraxellaceae and Xanthomonadaceae only encode for
355 cobamide biosynthesis genes cobP/cobU and cobS (Figure 6), which function in salvaging
356 cobinamide from the environment [44]. This suggests that in addition to specific taxa producing
357 cobamides *de novo*, there are other taxa that synthesize complete cobamides through salvaging
358 cobamide precursors from the environment. In addition, certain taxa, such as Veillonellaceae,
359 encode for adenosylcobinamide amidohydrolase CbiZ, which is involved in remodeling
360 cobamides with a new lower ligand [44,45]. Most predicted cobamide producers identified in this
361 analysis likely synthesize benzimidazole cobamides because they encode for bluB, the gene
362 responsible for the aerobic synthesis of lower ligand 5,6-dimethylbenzimidazole (DMB) (Figure 6)
363 [46–48]. Therefore, the identification of taxa that encode for cobamide remodeling enzymes
364 suggests that structurally distinct cobamides are produced and used for microbial metabolism on
365 the skin. Overall, these results demonstrate that certain skin taxa have the genetic potential to

366 produce complete cobamides through *de novo* biosynthesis, precursor salvage, or lower ligand
367 remodeling.
368

369 **Phylogenetically diverse skin taxa encode for cobamide-dependent enzymes and**
370 **cobalamin riboswitches.**
371 Our findings suggest that several taxa within the skin microbiome synthesize cobamides *de novo*.
372 Therefore, cobamides and cobamide precursors are likely available in the community for uptake
373 and use. To evaluate the potential utilization of cobamides by other taxa of the skin microbiome,
374 we searched 906 skin metagenomes for the cobamide transport protein btuB and 19 other
375 enzymes that carry out diverse cobamide dependent reactions (Supplemental Material S3). While
376 the total number of cobamide-dependent gene hits varied by microenvironment
377 (sebaceous=174,096, moist=70,994, dry=66,599, foot=45,412) (Supplemental Material S5), the
378 relative proportion of taxa encoding the genes was similar across microenvironments (Figure 7A).
379 Across sebaceous, moist, and dry microenvironments, Propionibacteriaecae was the dominant
380 taxa encoding for cobamide-dependent enzymes D-ornithine aminomutase, methylmalonyl-CoA
381 mutase, and ribonucleotide reductase class II, with this taxon contributing overall the most
382 cobamide-dependent sequences within the dataset (Supplemental Table S7). In contrast, we
383 found across the remaining cobamide-dependent enzymes, hits were assigned to
384 phylogenetically diverse taxa across the four major phyla on the skin (Actinobacteria, Firmicutes,
385 Proteobacteria, and Bacteroidetes) [17]. In particular, cobamide-dependent methionine synthase,
386 epoxyqueosine reductase, ethanolamine lyase, and ribonucleotide reductase were the most
387 common cobamide-dependent enzymes in the dataset, when considering the number of unique
388 taxa that encode for these enzymes (Supplemental Figure 3A). Notably, more unique species
389 within the dataset encode for at least one cobamide-dependent enzyme (n=456 species
390 contributing at least five reads to any cobamide-dependent enzyme) than appear to appreciably
391 contribute to *de novo* cobamide biosynthesis on the skin (n=23 species contributing at least five
392 reads to at least 7/10 biosynthesis genes) (Supplemental Table S9). This supports a model for
393 cobamide sharing, where a much larger number of skin taxa require cobamides than can produce
394 the cofactor *de novo*.
395

396 Cobalamin riboswitches are elements found in bacterial mRNAs that regulate expression of
397 cobamide-related transcripts through cobamide binding [49–51]. To further validate the use of
398 cobamides within the skin microbiome, we searched the skin metagenomes for cobalamin

399 riboswitches from the Rfam clan CL00101 (Supplemental Material S4). Similar to the cobamide
400 biosynthesis and cobamide-dependent gene analyses, phylogenetically diverse skin taxa encode
401 for cobalamin riboswitches, with Propionibacteriaceae being the dominant taxa. (Figure 7B). At
402 the species level, these hits were shown to be contributed predominantly by *Cutibacterium acnes*
403 (Supplemental Material S8).
404
405 To further explore the observed role that cobamides play in *C. acnes*, we mapped the identified
406 riboswitch metagenomic reads to the *C. acnes* KPA171202 reference genome and found that the
407 reads mapped to several genomic regions, with nearby genes having functions involved in ABC
408 transport, cobalt transport, cobamide biosynthesis, and cobamide-dependent and -independent
409 reactions (Figure 8A). Regions 6, 7, and 8 did not encode for known cobamide-related genes, but
410 all were found directly upstream of a small ~250 bp pseudogene and either a 1321 bp pseudogene
411 (Region 6) or 1922 bp hypothetical protein (Regions 7 and 8). BLAST searches of the sequences
412 revealed that the small pseudogenes are hypothetical adhesin protein fragments and the larger
413 sequences that directly follow are thrombospondin type-3 repeat containing proteins
414 (Supplemental Material S10). The role of cobalamin riboswitches in regulating these sequences
415 is not clear. We also mapped the riboswitch-containing reads to the genomes of other skin taxa,
416 finding that there were overall fewer cobalamin riboswitches within these genomes compared to
417 *C. acnes*, but were similarly found nearby to genes with functions in cobamide biosynthesis, ABC
418 transport, cobalt transport, and both cobamide-dependent and cobamide-independent isozymes
419 (Figure 8B, C, D, E). Thus, within the skin microbiome, cobalamin riboswitches are likely to
420 regulate diverse processes, including those that may not currently be characterized.
421
422 **DISCUSSION**
423
424 *Corynebacterium* species are well-equipped for growth on the skin due to their "lipid-loving" and
425 halotolerant nature, allowing them to thrive in moist and sebaceous skin microenvironments [52].
426 However, many questions remain about the processes that govern skin colonization by this
427 relatively understudied skin taxa and how these processes may impact or be impacted by
428 microbe-microbe and microbe-host interactions on the skin.
429
430 Our *Corynebacterium* comparative genomics analysis revealed that host-associated
431 Corynebacteria have significantly smaller genomes compared to environment-associated
432 genomes and further, that distinct functions are enriched between the two groups (Figure 2). For

433 free-living microorganisms like EA Corynebacteria, selection likely drives the retention of
434 metabolic functions, presumably due to inconsistent availability of certain nutrients and other
435 compounds in the environment [53]. Whereas in microorganisms in association with a host, the
436 host provides a relatively consistent supply of nutrients and metabolic intermediates, therefore
437 eliminating the pressure to retain certain metabolic functions, leading to gene loss over time
438 [54]. Therefore, we predict that the reduced genome size of HA *Corynebacterium* species arose
439 from loss of metabolic functions, which is supported by the observation that EA genomes are
440 enriched in functions associated with diverse substrate metabolism. A rather unexpected finding
441 from our study was the enrichment of *de novo* cobamide biosynthesis within HA genomes.
442 Retention of the energetically costly 25-enzyme cobamide biosynthesis pathway within HA
443 *Corynebacterium* species, even with reduced genome size, suggests that synthesis of this
444 cofactor is advantageous for host niche colonization.
445
446 While decades-old literature have implicated *Corynebacterium* species in *de novo* cobamide
447 biosynthesis [55–57], only a few recent studies have explored this relatively rare function by
448 members of the genus [31,58–60]. Here, we demonstrate that within the *Corynebacterium* genus,
449 the *de novo* cobamide biosynthesis pathway is conserved among specific lineages, including
450 those that contain skin-associated species (Figure 3). However, the existence of other lineages
451 that do not encode for the complete suite of genes required for biosynthesis suggests that there
452 has been evolutionary pressure for either retention or loss of the pathway. The presence of
453 remnant cobamide biosynthesis genes within the *C. glutamicum* clade and the conserved nature
454 of cobU/cobT and cobC throughout the genus, which are currently known to only function in
455 cobamide biosynthesis [61–63], supports the likelihood of pathway loss.
456
457 A key question that arises is why some *Corynebacterium* species have retained the *de novo*
458 cobamide biosynthesis pathway, while others have not. From our analysis of skin metagenomes,
459 we observed reads encoding for cobamide-dependent methionine synthase, methylmalonyl-CoA
460 mutase, and ethanolamine ammonia lyase from the *Corynebacterium* genus, which is consistent
461 with previous findings by Shelton *et al.* [31]. Therefore, cobamides are likely produced to fulfill
462 metabolic requirements in methionine, propionate, and glycerophospholipid metabolism in
463 Corynebacteria. Alternative cobamide-independent pathways exist for these functions, therefore
464 cobamides may confer a distinct advantage for *Corynebacterium* cobamide-producing species.
465 Indeed, metE, the cobamide-independent methionine synthase, is sensitive to oxidative stress
466 and has reduced turnover compared to metH [64–66]. The skin in particular is subject to high

467 oxidative stress as a result of metabolic reactions, cosmetics, and UV irradiation exposure. [67–
468 69]. Therefore, while the significance of employing cobamide-dependent vs -independent
469 isozymes for bacterial metabolism on the skin is unknown, inherent features of the skin such as
470 high oxidative stress may play a role.
471
472 While other studies of cobamides in microbial communities have demonstrated that *de novo*
473 synthesis is carried out by a relatively small fraction of the community [33,70,71], our analysis of
474 skin metagenomic data suggests that on the skin, cobamides are produced by taxa considered
475 dominant within the microbiome, including *Cutibacterium* and *Corynebacterium* species. We
476 identified that overall, *C. acnes* is the top cobamide producer and user within our dataset and is
477 likely under tight regulation of cobamide biosynthesis and cobamide-dependent enzyme
478 expression by more than 10 cobalamin riboswitches. Indeed, cobalamin riboswitch regulation has
479 been demonstrated to decrease expression of *C. acnes* cobamide biosynthesis genes in the
480 presence of exogenous vitamin B_{12}, both *in vitro* and on the skin of healthy individuals [72]. We
481 also identified that three of the *C. acnes* cobalamin riboswitches are located upstream of proteins
482 containing thrombospondin type 3 repeats (TT3Rs), which are efficient calcium ion binding motifs
483 that have been well-studied in eukaryotes, but not prokaryotes [73]. TT3Rs that have been
484 investigated in prokaryotes have been associated with the outer membrane of Gram-negative
485 bacteria, therefore in the Gram-positive *C. acnes*, the role for TT3R-containing proteins is
486 unknown and likely distinct. We predict that on the skin, cobalamin riboswitches could regulate
487 functions not currently characterized to have a cobamide association.
488
489 Interestingly, we observed that other predicted cobamide producers on the skin, including *V.*
490 *parvula* and *Corynebacterium* sp. ATCC 6931, only possess a few cobalamin riboswitches, and
491 these riboswitches appear to regulate cobamide-dependent and -independent functions and ABC
492 transport, as opposed to cobamide biosynthesis. This could suggest a more constitutive
493 expression of cobamide biosynthesis by certain skin taxa, providing a possible explanation for the
494 observed increase in microbiome diversity with cobamide-producing Corynebacteria as compared
495 to the low diversity communities with high *C. acnes* abundance. Overall, cobamide production
496 and riboswitch regulation are likely to act as mediators of microbe-microbe interactions on the
497 skin.
498
499 In support of a key role for cobamides within the skin microbiome, we found that other
500 phylogenetically diverse skin taxa, both dominant and low abundance, encode for metabolically

501 diverse cobamide-dependent enzymes, as well as proteins involved in cobamide transport,
502 salvage, and remodeling (Figures 6 and 7). Because cobamide structure can dictate microbial
503 growth and metabolism [74], microorganisms exhibit cobamide selectivity, employing numerous
504 mechanisms for acquiring and using their preferred cobamide(s). These include selectivity in
505 cobamide-dependent enzymes, differential cobamide import, and cobamide-specific gene
506 regulation [74]. While cobamides are not likely to be scarce on the skin based on the observation
507 that dominant taxa encode for *de novo* biosynthesis, the specific cobamides required for skin
508 microbial metabolism is unknown. The presence of cobamide remodeling enzyme cbiZ, which is
509 encoded by some skin taxa, may serve as an indicator that certain skin bacteria use cobamide-
510 dependent enzymes with specific lower ligand preferences [45], thus implicating a role for
511 cobamide salvaging and sharing within the skin microbiome in fulfilling metabolic requirements.
512
513 Within microbial communities, cobamides are hypothesized to mediate community dynamics
514 because of the relative paucity of cobamide producers, yet evident requirement for this cofactor
515 across the bacterial domain of life [31,74,75]. Our results suggest that on the skin,
516 *Corynebacterium* cobamide-producing species may promote microbiome diversity (Figure 4)
517 through an increase in community alpha diversity that arises from an overall more evenly
518 distributed community. Interestingly, we observed that communities with low abundance of
519 cobamide-producing Corynebacteria and thus low diversity were dominated by *Propionibacterium*
520 species, predicted to be the dominant cobamide producer on the skin. Because we anticipate
521 communities that produce more cobamides to have increased diversity, this result is confounding.
522 However, because a spectrum of ecological niches exists on the skin, ranging from the anaerobic
523 sebaceous follicle to the aerobic and desiccate skin surface, we hypothesize that cobamide
524 interactions are dependent upon spatial structure of skin microbial communities. For example, *C.*
525 *acnes* is an anaerobe that predominantly resides deep within the anaerobic sebaceous follicle
526 [76], dominating between 60-90% of the follicle community [77]. As such, the opportunity for
527 cobamide-mediated interactions is likely reduced as a result of the *C. acnes*-dominated
528 sebaceous gland. Approaching the more oxygenated skin surface, the community becomes more
529 diverse [18], thus increasing the incidence of cobamide interactions and subsequent effects on
530 community dynamics. Furthermore, *C. acnes* and other related *Cutibacterium* and
531 *Propionibacterium* species produce cobamides with DMB as the lower ligand, requiring the bluB
532 gene. However, the bluB reaction must proceed under aerobic conditions. How *C. acnes*
533 synthesizes complete cobamides within the anaerobic sebaceous follicle is unknown, but
534 suggests a possible role for DMB sharing within the skin microbiome.

535

536 Overall, our findings reveal that skin-associated species within the *Corynebacterium* genus
537 encode for the *de novo* cobamide biosynthesis pathway, which is a relatively rare metabolic
538 function. Within skin microbial communities, abundance of these cobamide-producing
539 Corynebacteria is correlated with increased microbiome diversity, suggesting that cobamides are
540 important mediators of microbiome structure. We also demonstrate that cobamide use is
541 widespread across phylogenetically diverse skin taxa, therefore we hypothesize that cobamides
542 are likely to play a significant role in skin microbial community dynamics. Future studies to
543 interrogate cobamide interactions between skin commensals will provide insight into the effects
544 of cobamide biosynthesis and use within microbial communities.
545

546 **REFERENCES**

547 1. Scharschmidt TC, Vasquez KS, Pauli ML, Leitner EG, Chu K, Truong HA, et al.
548 Commensal Microbes and Hair Follicle Morphogenesis Coordinately Drive Treg Migration
549 into Neonatal Skin. Cell Host Microbe. 2017. doi:10.1016/j.chom.2017.03.001

550 2. Constantinides MG, Link VM, Tamoutounour S, Wong AC, Perez-Chaparro PJ, Han S-J,
551 et al. MAIT cells are imprinted by the microbiota in early life and promote tissue repair.
552 Science. 2019;366. doi:10.1126/science.aax6624

553 3. Linehan JL, Harrison OJ, Han S-J, Byrd AL, Vujkovic-Cvijin I, Villarino AV, et al. Non-
554 classical Immunity Controls Microbiota Impact on Skin Immunity and Tissue Repair. Cell.
555 2018;172: 784–796.e18.

556 4. Belkaid Y, Harrison OJ. Homeostatic Immunity and the Microbiota. Immunity. 2017;46:
557 562–576.

558 5. Di Domizio J, Belkhodja C, Chenuet P, Fries A, Murray T, Mondéjar PM, et al. The
559 commensal skin microbiota triggers type I IFN-dependent innate repair responses in
560 injured skin. Nat Immunol. 2020;21: 1034–1045.

561 6. Wanke I, Steffen H, Christ C, Krismer B, Götz F, Peschel A, et al. Skin commensals
562 amplify the innate immune response to pathogens by activation of distinct signaling
563 pathways. J Invest Dermatol. 2011;131: 382–390.

564 7. Claesen J, Spagnolo JB, Ramos SF, Kurita KL, Byrd AL, Aksenov AA, et al. A
565 Cutibacterium acnes antibiotic modulates human skin microbiota composition in hair
566 follicles. Sci Transl Med. 2020;12. doi:10.1126/scitranslmed.aay5445

567 8. Oh J, Byrd AL, Park M, Kong HH, Segre JA. Temporal Stability of the Human Skin
568 Microbiome. Cell. 2016;165: 854–866.

569 9. Tomida S, Nguyen L, Chiu B-H, Liu J, Sodergren E, Weinstock GM, et al. Pan-genome
570 and comparative genome analyses of propionibacterium acnes reveal its genomic diversity
571 in the healthy and diseased human skin microbiome. MBio. 2013;4: e00003–13.

572 10. Wollenberg MS, Claesen J, Escapa IF, Aldridge KL, Fischbach MA, Lemon KP.
573 Propionibacterium-produced coproporphyrin III induces Staphylococcus aureus
574 aggregation and biofilm formation. MBio. 2014;5: e01286–14.

575 11. Christensen GJM, Scholz CFP, Enghild J, Rohde H, Kilian M, Thürmer A, et al.
576 Antagonism between Staphylococcus epidermidis and Propionibacterium acnes and its
577 genomic basis. BMC Genomics. 2016;17: 152.

578 12. O'Sullivan JN, Rea MC, O'Connor PM, Hill C, Ross RP. Human skin microbiota is a rich
579 source of bacteriocin-producing staphylococci that kill human pathogens. FEMS Microbiol
580 Ecol. 2019;95. doi:10.1093/femsec/fiy241

581 13. Nakatsuji T, Chen TH, Narala S, Chun KA, Two AM, Yun T, et al. Antimicrobials from
582 human skin commensal bacteria protect against Staphylococcus aureus and are deficient
583 in atopic dermatitis. Sci Transl Med. 2017;9. doi:10.1126/scitranslmed.aah4680

584 14. Naik S, Bouladoux N, Wilhelm C, Molloy MJ, Salcedo R, Kastenmuller W, et al.
585 Compartmentalized control of skin immunity by resident commensals. Science. 2012;337:
586 1115–1119.

587 15. Gallo RL, Nakatsuji T. Microbial symbiosis with the innate immune defense system of the
588 skin. J Invest Dermatol. 2011;131: 1974–1980.

589 16. Brandwein M, Bentwich Z, Steinberg D. Endogenous Antimicrobial Peptide Expression in
590 Response to Bacterial Epidermal Colonization. Front Immunol. 2017;8: 1637.

591 17. Grice EA, Segre JA. The skin microbiome. Nat Rev Microbiol. 2011;9: 244–253.

592 18. Oh J, Byrd AL, Deming C, Conlan S, NISC Comparative Sequencing Program, Kong HH,
593 et al. Biogeography and individuality shape function in the human skin metagenome.
594 Nature. 2014;514: 59–64.

595 19. Grice EA, Kong HH, Conlan S, Deming CB, Davis J, Young AC, et al. Topographical and
596 temporal diversity of the human skin microbiome. Science. 2009;324: 1190–1192.

597 20. Bomar L, Brugger SD, Yost BH, Davies SS, Lemon KP. Corynebacterium accolens
598 Releases Antipneumococcal Free Fatty Acids from Human Nostril and Skin Surface
599 Triacylglycerols. MBio. 2016;7: e01725–15.

600 21. Ramsey MM, Freire MO, Gabrilska RA, Rumbaugh KP, Lemon KP. Staphylococcus
601 aureus Shifts toward commensalism in response to corynebacterium species. Front
602 Microbiol. 2016. doi:10.3389/fmicb.2016.01230

603 22. Altonsy MO, Kurwa HA, Lauzon GJ, Amrein M, Gerber AN, Almishri W, et al.
604 Corynebacterium tuberculostearicum, a human skin colonizer, induces the canonical
605 nuclear factor-κB inflammatory signaling pathway in human skin cells. Immun Inflamm Dis.
606 2020;8: 62–79.

607 23. Ridaura VK, Bouladoux N, Claesen J, Chen YE, Byrd AL, Constantinides MG, et al.
608 Contextual control of skin immunity and inflammation by Corynebacterium. J Exp Med.
609 2018;215: 785–799.

610 24. Eren AM, Esen OC, Quince C, Vineis JH, Morrison HG, Sogin ML, et al. Anvi'o: An
611 advanced analysis and visualization platformfor 'omics data. PeerJ. 2015;2015: e1319.

612 25. Delmont TO, Murat Eren A. Linking pangenomes and metagenomes: the Prochlorococcus
613 metapangenome. PeerJ. 2018. p. e4320. doi:10.7717/peerj.4320

614 26. Pritchard L, Glover RH, Humphris S, Elphinstone JG, Toth IK. Genomics and taxonomy in
615 diagnostics for food security: soft-rotting enterobacterial plant pathogens. Anal Methods.
616 2015;8: 12–24.

617 27. Edgar RC. MUSCLE: multiple sequence alignment with high accuracy and high
618 throughput. Nucleic Acids Res. 2004;32: 1792–1797.

619 28. Price MN, Dehal PS, Arkin AP. FastTree 2--approximately maximum-likelihood trees for
620 large alignments. PLoS One. 2010;5: e9490.

621 29. Aramaki T, Blanc-Mathieu R, Endo H, Ohkubo K, Kanehisa M, Goto S, et al.
622 KofamKOALA: KEGG Ortholog assignment based on profile HMM and adaptive score
623 threshold. Bioinformatics. 2020;36: 2251–2252.

624 30. Yu G, Smith DK, Zhu H, Guan Y, Lam TT. ggtree : an r package for visualization and
625 annotation of phylogenetic trees with their covariates and other associated data. McInerny
626 G, editor. Methods Ecol Evol. 2017;8: 28–36.

627 31. Shelton AN, Seth EC, Mok KC, Han AW, Jackson SN, Haft DR, et al. Uneven distribution
628 of cobamide biosynthesis and dependence in bacteria predicted by comparative
629 genomics. ISME J. 2019;13: 789–804.

630 32. Doxey AC, Kurtz DA, Lynch MDJ, Sauder LA, Neufeld JD. Aquatic metagenomes
631 implicate Thaumarchaeota in global cobalamin production. ISME J. 2015;9: 461–471.

632 33. Lu X, Heal KR, Ingalls AE, Doxey AC, Neufeld JD. Metagenomic and chemical
633 characterization of soil cobalamin production. ISME J. 2020;14: 53–66.

634 34. Rice P, Longden I, Bleasby A. EMBOSS: the European Molecular Biology Open Software
635 Suite. Trends Genet. 2000;16: 276–277.

636 35. Eddy SR. Accelerated profile HMM searches. PLoS Comput Biol. 2011;7: 1002195.

637 36. Wood DE, Lu J, Langmead B. Improved metagenomic analysis with Kraken 2. Genome
638 Biol. 2019;20: 257.

639 37. Lu J, Breitwieser FP, Thielen P, Salzberg SL. Bracken: Estimating species abundance in
640 metagenomics data. PeerJ Computer Science. 2017;2017: e104.

641 38. Kalvari I, Argasinska J, Quinones-Olvera N, Nawrocki EP, Rivas E, Eddy SR, et al. Rfam
642 13.0: shifting to a genome-centric resource for non-coding RNA families. Nucleic Acids
643 Res. 2018;46: D335–D342.

644 39. Nawrocki EP, Eddy SR. Infernal 1.1: 100-fold faster RNA homology searches.
645 BIOINFORMATICS APPLICATIONS. 2013;29: 2933–2935.

646 40. Pascual C, Lawson PA, Farrow JA, Gimenez MN, Collins MD. Phylogenetic analysis of the
647 genus Corynebacterium based on 16S rRNA gene sequences. Int J Syst Bacteriol.
648 1995;45: 724–728.

649 41. Pollich M, Klug G. Identification and sequence analysis of genes involved in late steps in
650 cobalamin (vitamin B12) synthesis in Rhodobacter capsulatus. J Bacteriol. 1995;177:
651 4481–4487.

652 42. Fang H, Kang J, Zhang D. Microbial production of vitamin B12: a review and future
653 perspectives. Microb Cell Fact. 2017;16: 15.

654 43. Hazra AB, Tran JLA, Crofts TS, Taga ME. Analysis of substrate specificity in CobT
655 homologs reveals widespread preference for DMB, the lower axial ligand of vitamin B(12).
656 Chem Biol. 2013;20: 1275–1285.

657 44. Gray MJ, Tavares NK, Escalante-Semerena JC. The genome of Rhodobacter sphaeroides
658 strain 2.4.1 encodes functional cobinamide salvaging systems of archaeal and bacterial
659 origins. Mol Microbiol. 2008;70: 824–836.

660 45. Gray MJ, Escalante-Semerena JC. The cobinamide amidohydrolase (cobyric acid-forming)
661 CbiZ enzyme: a critical activity of the cobamide remodelling system of *Rhodobacter*
662 *sphaeroides*. Mol Microbiol. 2009;74: 1198–1210.

663 46. Taga ME, Larsen NA, Howard-Jones AR, Walsh CT, Walker GC. BluB cannibalizes flavin
664 to form the lower ligand of vitamin B12. Nature. 2007;446: 449–453.

665 47. Campbell GRO, Taga ME, Mistry K, Lloret J, Anderson PJ, Roth JR, et al. Sinorhizobium
666 meliloti bluB is necessary for production of 5,6-dimethylbenzimidazole, the lower ligand of
667 B12. Proc Natl Acad Sci U S A. 2006;103: 4634–4639.

668 48. Gray MJ, Escalante-Semerena JC. Single-enzyme conversion of FMNH2 to 5,6-
669 dimethylbenzimidazole, the lower ligand of B12. Proc Natl Acad Sci U S A. 2007;104:
670 2921–2926.

671 49. Garst AD, Edwards AL, Batey RT. Riboswitches: Structures and mechanisms. Cold Spring
672 Harbor Perspectives in Biology. Cold Spring Harbor Laboratory Press; 2011. pp. 1–13.
673 doi:10.1101/cshperspect.a003533

674 50. Nahvi A, Barrick JE, Breaker RR. Coenzyme B12 riboswitches are widespread genetic
675 control elements in prokaryotes. Nucleic Acids Res. 2004;32: 143–150.

676 51. Polaski JT, Webster SM, Johnson JE, Batey RT. Cobalamin riboswitches exhibit a broad
677 range of ability to discriminate between methylcobalamin and adenosylcobalamin. J Biol
678 Chem. 2017;292: 11650–11658.

679 52. Scharschmidt TC, Fischbach MA. What Lives On Our Skin: Ecology, Genomics and
680 Therapeutic Opportunities Of the Skin Microbiome. Drug Discov Today Dis Mech.
681 2013;10. doi:10.1016/j.ddmec.2012.12.003

682 53. Wernegreen JJ. Endosymbiont evolution: predictions from theory and surprises from
683 genomes. Ann N Y Acad Sci. 2015;1360: 16–35.

684 54. Moran NA. Tracing the evolution of gene loss in obligate bacterial symbionts. Curr Opin
685 Microbiol. 2003;6: 512–518.

686 55. Perlman D. Microbial Synthesis of Cobamides11Presented in part in lectures before
687 School of Pharmacy, University of Wisconsin, March, 1958. In: Umbreit WW, editor.
688 Advances in Applied Microbiology. Academic Press; 1959. pp. 87–122.

689 56. Andriantsoa M, Laget M, Cremieux A, Dumenil G. Constant fed-batch culture of methanol-
690 utilizing corynebacterium producing vitamin B 12. Biotechnol Lett. 1984;6: 783–788.

691 57. Fujii K, Takeuchi H, Shimizu S, Fukui S. Vitamin B12-dependent Methionine Biosynthesis
692 and Its Metabolic Role in Corynebacterium simplex ATCC 6946, a Vitamin B12-producing
693 and Hydrocarbon-utilizable Bacterium. Agric Biol Chem. 1972;36: 2323–2334.

694 58. dos S. Peinado R, Olivier DS, Eberle RJ, de Moraes FR, Amaral MS, Arni RK, et al.
695 Binding studies of a putative C . pseudotuberculosis target protein from Vitamin B 12
696 Metabolism. Sci Rep. 2019;9: 1–13.

697 59. Al-Dilaimi A, Albersmeier A, Kalinowski J, Rückert C. Complete genome sequence of
698 Corynebacterium vitaeruminis DSM 20294T, isolated from the cow rumen as a vitamin B
699 producer. J Biotechnol. 2014;189: 70–71.

700 60. Antonov IV. Two cobalt chelatase subunits can be generated from a single chlD gene via
701 programmed frameshifting. Mol Biol Evol. 2020. Available:
702 https://academic.oup.com/mbe/article-abstract/doi/10.1093/molbev/msaa081/5811573

703 61. Zayas CL, Escalante-Semerena JC. Reassessment of the late steps of coenzyme B12
704 synthesis in Salmonella enterica: evidence that dephosphorylation of adenosylcobalamin-
705 5'-phosphate by the CobC phosphatase is the last step of the pathway. J Bacteriol.
706 2007;189: 2210–2218.

707 62. O'Toole GA, Trzebiatowski JR, Escalante-Semerena JC. The cobC gene of Salmonella
708 typhimurium codes for a novel phosphatase involved in the assembly of the nucleotide
709 loop of cobalamin. J Biol Chem. 1994;269: 26503–26511.

710 63. Cheong C-G, Escalante-Semerena JC, Rayment I. The three-dimensional structures of
711 nicotinate mononucleotide: 5, 6-dimethylbenzimidazole phosphoribosyltransferase (CobT)
712 from Salmonella typhimurium complexed with 5, 6-dimethybenzimidazole and its reaction
713 products determined to 1.9 Å resolution. Biochemistry. 1999;38: 16125–16135.

714 64. González JC, Banerjee RV, Huang S, Sumner JS, Matthews RG. Comparison of
715 cobalamin-independent and cobalamin-dependent methionine synthases from Escherichia
716 coli: two solutions to the same chemical problem. Biochemistry. 1992;31: 6045–6056.

717 65. Hondorp ER, Matthews RG. Oxidative stress inactivates cobalamin-independent
718 methionine synthase (MetE) in Escherichia coli. PLoS Biol. 2004;2: e336.

719 66. Leichert LI, Jakob U. Protein thiol modifications visualized in vivo. PLoS Biol. 2004;2:
720 e333.

721 67. Andersson T, Ertürk Bergdahl G, Saleh K, Magnúsdóttir H, Stødkilde K, Andersen CBF, et
722 al. Common skin bacteria protect their host from oxidative stress through secreted
723 antioxidant RoxP. Sci Rep. 2019;9: 3596.

724 68. Kawashima S, Funakoshi T, Sato Y, Saito N, Ohsawa H, Kurita K, et al. Protective effect
725 of pre- and post-vitamin C treatments on UVB-irradiation-induced skin damage. Sci Rep.
726 2018;8: 16199.

727 69. Hakozaki T, Date A, Yoshii T, Toyokuni S, Yasui H, Sakurai H. Visualization and
728 characterization of UVB-induced reactive oxygen species in a human skin equivalent
729 model. Arch Dermatol Res. 2008;300 Suppl 1: S51–6.

730 70. Magnúsdóttir S, Ravcheev D, de Crécy-Lagard V, Thiele I. Systematic genome
731 assessment of B-vitamin biosynthesis suggests co-operation among gut microbes. Front
732 Genet. 2015;6: 148.

733 71. Romine MF, Rodionov DA, Maezato Y, Osterman AL, Nelson WC. Underlying
734 mechanisms for syntrophic metabolism of essential enzyme cofactors in microbial
735 communities. ISME J. 2017;11: 1434–1446.

736 72. Kang D, Shi B, Erfe MC, Craft N, Li H. Vitamin B 12 modulates the transcriptome of the
737 skin microbiota in acne pathogenesis. Sci Transl Med. 2015;7: 293ra103–293ra103.

738 73. Dai S, Sun C, Tan K, Ye S, Zhang R. Structure of thrombospondin type 3 repeats in
739 bacterial outer membrane protein A reveals its intra-repeat disulfide bond-dependent
740 calcium-binding capability. Cell Calcium. 2017;66: 78–89.

741 74. Sokolovskaya OM, Shelton AN, Taga ME. Sharing vitamins: Cobamides unveil microbial
742 interactions. Science. 2020;369: eaba0165.

743 75. Degnan Patrick H. Taga Michiko E. Goodman AL. Vitamin B12 as a modulator of gut
744 microbial ecology. Cell Metab. 2014;20: 1–769–778.

745 76. Dréno B, Pécastaings S, Corvec S, Veraldi S, Khammari A, Roques C. Cutibacterium
746 acnes (Propionibacterium acnes) and acne vulgaris: a brief look at the latest updates. J
747 Eur Acad Dermatol Venereol. 2018;32: 5–14.

748 77. Hall JB, Cong Z, Imamura-Kawasawa Y, Kidd BA, Dudley JT, Thiboutot DM, et al.
749 Isolation and Identification of the Follicular Microbiome: Implications for Acne Research. J
750 Invest Dermatol. 2018;138: 2033–2040.

751 78. Hannigan GD, Meisel JS, Tyldsley AS, Zheng Q, Hodkinson BP, SanMiguel AJ, et al. The
752 human skin double-stranded DNA virome: topographical and temporal diversity, genetic
753 enrichment, and dynamic associations with the host microbiome. MBio. 2015;6: e01578–
754 15.
755

FIGURE LEGENDS

Figure 1. *Corynebacterium* pangenome. Pangenome analysis generated with anvi'o. 42,154 gene clusters (combined core, dispensable, and singletons) were identified from 71 *Corynebacterium* genomes and are ordered by gene cluster frequency (opaque, present; transparent, absent). Each gene cluster contains one or more genes contributed by one or more genomes. Genomes are colored by ecosystem association and ordered by the phylogeny based on 71 single copy genes (unrooted). ANI scale (0.7-0.8). Singleton gene clusters (grey) are collapsed.

Figure 2. Host- and environment-associated *Corynebacterium* genomes have distinct genetic features. A) Genome length and B) number of gene clusters for 71 *Corynebacterium* genomes was determined using anvi'o. Significance was determined using Tukey's Test for post hoc analysis. C) Significantly enriched COG functions in C) host-associated or D) environment-associated genomes were identified with anvi'o. The top 20 significantly enriched COG functions ($q < 0.05$) are shown, ordered by ascending significance. Blue = host-associated, orange = environment-associated.

Figure 3. *De novo* cobamide biosynthesis is host-associated within the *Corynebacterium* genus. A *Corynebacterium* phylogenetic tree based on comparison of 71 conserved single copy genes was generated using FastTree within the anvi'o environment. The tree is rooted with *Tsukamurella paurometabola*. Species are colored by host (blue) or environment (orange) association, and by genome length (dark blue). KOfamScan was used to identify the presence (dark pink) or absence (light pink) of cobamide biosynthesis genes within each genome. Cobamide biosynthesis is separated into tetrapyrrole precursor, corrin ring, nucleotide loop, and lower ligand synthesis.

Figure 4. Microbiome diversity is associated with abundance of cobamide-producing *Corynebacterium* species. Within each metagenome, the total abundance of 5 cobamide-producing *Corynebacterium* (CPC) species was calculated. A) CPC abundance is plotted against the Shannon diversity indices for samples within each skin site. R=Spearman's correlation coefficient. B) NMDS plots based on Bray-Curtis indices for samples within each skin site are shown. Points are colored by log 10 *Corynebacterium* cobamide producer abundance and sized by alpha diversity (Shannon).

790 **Figure 5. Taxonomic contribution of cobamide biosynthesis genes across skin sites is site-**
791 **dependent.** For each taxa shown, the number of cobamide biosynthesis gene hits (normalized
792 by profile HMM coverages) assigned to the given taxa was divided by the overall total number
793 of cobamide biosynthesis gene hits within the sample. Taxon contributions are shown for the top
794 5 taxa with the most cobamide biosynthesis gene hits, grouped by skin site. Color indicates
795 microenvironment classification.
796
797 **Figure 6. Many skin taxa encode for genes required for *de novo* cobamide biosynthesis.**
798 The top 40 abundant taxa within the dataset were determined by totaling the hits to single copy
799 gene *rpoB* (normalized by profile HMM coverage). The remaining taxa were grouped into "Other".
800 Individual values in the heatmap represent the number of hits assigned to the taxon for a particular
801 cobamide biosynthesis gene divided by the total number of hits to the gene. Gene hits were
802 normalized by profile HMM coverage and sequencing depth prior to calculation.
803
804 **Figure 7. Phylogenetically diverse skin bacteria encode cobamide-dependent enzymes,**
805 **cobamide transporters, and cobalamin riboswitches** A) The total normalized hits for 17
806 cobamide-dependent enzymes and cobamide transport protein btuB are shown (totals hits
807 normalized to profile HMM coverage and sequence depth), with the taxonomic abundance of the
808 hits expanded above. Hits to distinct B12-dependent radical SAM proteins are grouped together
809 as "B12-dep radical SAM". B) The taxonomic abundance of hits for cobalamin riboswitches (Rfam
810 clan CL00101) are shown, with an expanded view of low abundance hits to the right. Total
811 cobalamin riboswitch hits within each microenvironment are indicated.
812
813 **Figure 8. Cobalamin riboswitches regulate diverse functions within skin bacteria.**
814 Cobalamin riboswitch-containing reads identified from INFERNAL analysis were aligned to A)
815 *Cutibacterium acnes* KPA171202, B) *Veillonella parvula* DSM 2008, C) *Pseudomonas putida*
816 KT2440, D) *Corynebacterium* sp. ATCC 6931, and E) *Streptococcus sanguinis* SK36 genomes.
817 Pink lines along the light grey genome track indicate the position of mapped INFERNAL hits within
818 the genome. Genes upstream and downstream of the riboswitches are colored by their general
819 functional annotation. White (unrelated) indicates genes not currently known to be associated
820 with cobamides. Grey (hypothetical) indicates a hypothetical protein that has no functional
821 annotation. Genomic regions are not to scale.
822
823

824 **SUPPLEMENTARY FIGURE LEGENDS**

825 **Supplementary Figure 1. *Corynebacterium* cobamide producer abundance vs. Richness.**
826 Within each metagenome, the total abundance of 5 cobamide-producing *Corynebacterium* (CPC)
827 species was calculated. CPC abundance is plotted against richness (observed species) for
828 samples within each skin site. R=Spearman's correlation coefficient.

829

830 **Supplementary Figure 2. Relative abundance of metagenomes with low or high**
831 ***Corynebacterium* cobamide producer abundance.** The first (0.05%) and third (0.5%) quartiles
832 of the cobamide-producing *Corynebacterium* (CPC) relative abundance across all samples were
833 used to group samples below 0.05% or above 0.5% CPC abundance. Relative abundances for
834 samples within each group are shown. Species less than 10% relative abundance are grouped
835 into "Other".

836

837 **Supplemental Figure 3. Number of unique species encoding for cobamide-dependent**
838 **enzymes, and cobalamin riboswitches.** For A) cobamide-dependent enzymes and B)
839 cobalamin riboswitches, the total number of unique species contributing at least 5 reads to each
840 gene were calculated.

841

842

Figure 1

Corynebacterium Pangenome

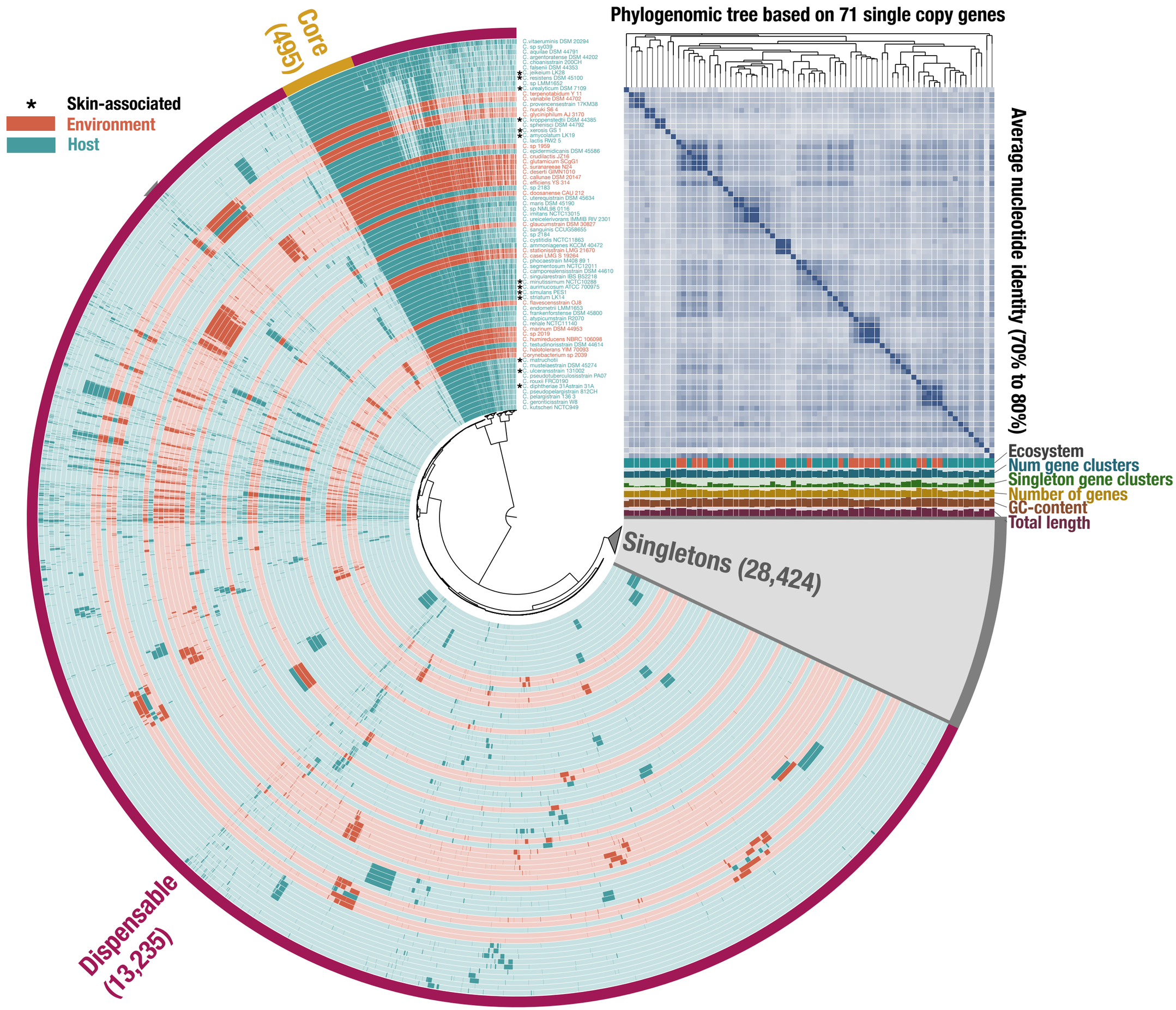

Figure 2

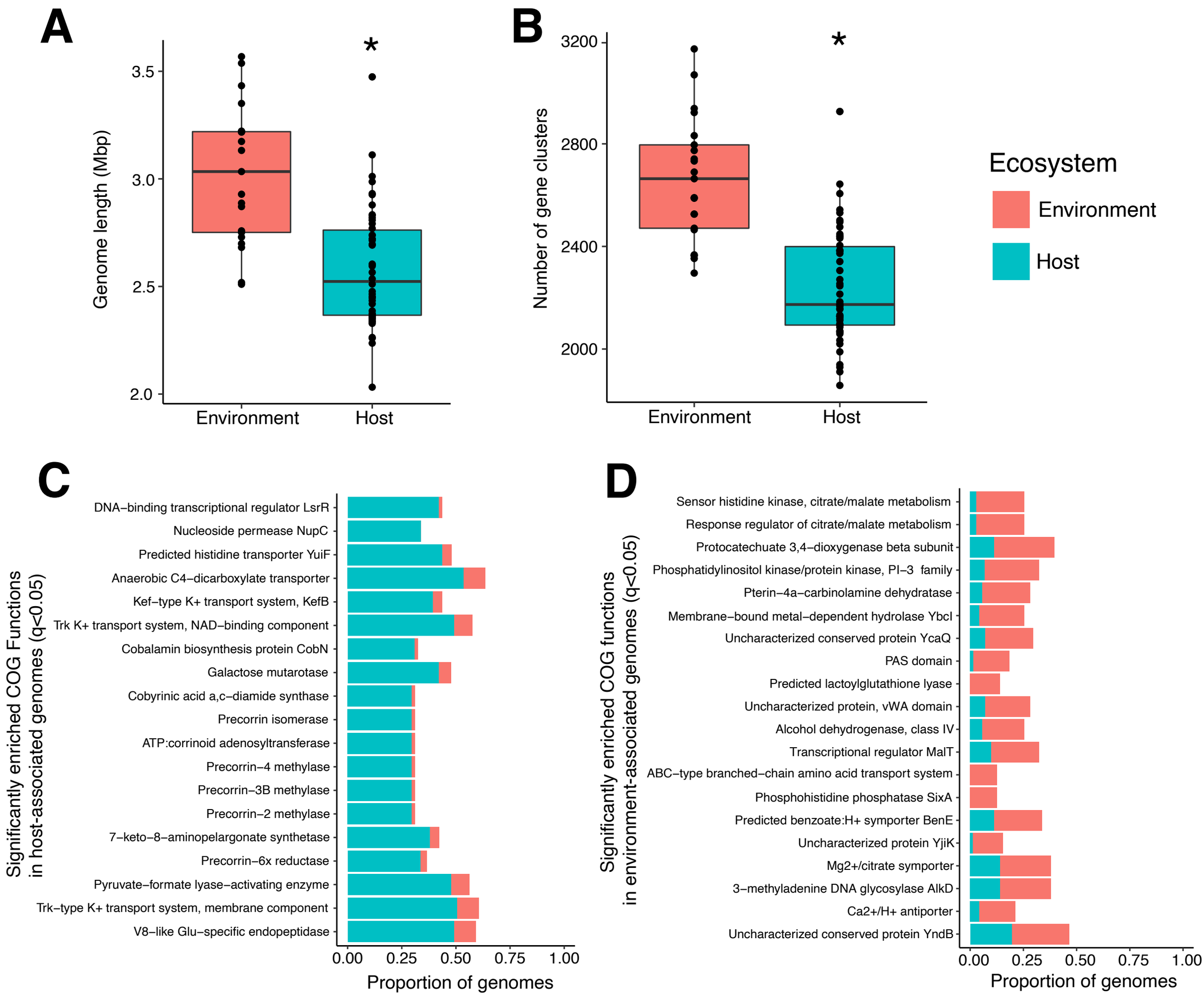
A
Genome length (Mbp)
3.5
3.0
2.5
2.0
*
Environment
Host
B
Number of gene clusters
3200
2800
2400
2000
*
Environment
Host
Ecosystem
Environment
Host
C
Significantly enriched COG Functions in host-associated genomes (q<0.05)
DNA−binding transcriptional regulator LsrR
Nucleoside permease NupC
Predicted histidine transporter YuiF
Anaerobic C4−dicarboxylate transporter
Kef−type K+ transport system, KefB
Trk K+ transport system, NAD−binding component
Cobalamin biosynthesis protein CobN
Galactose mutarotase
Cobyrinic acid a,c−diamide synthase
Precorrin isomerase
ATP:corrinoid adenosyltransferase
Precorrin−4 methylase
Precorrin−3B methylase
Precorrin−2 methylase
7−keto−8−aminopelargonate synthetase
Precorrin−6x reductase
Pyruvate−formate lyase−activating enzyme
Trk−type K+ transport system, membrane component
V8−like Glu−specific endopeptidase
0.00
0.25
0.50
0.75
1.00
Proportion of genomes
D
Significantly enriched COG functions in environment-associated genomes (q<0.05)
Sensor histidine kinase, citrate/malate metabolism
Response regulator of citrate/malate metabolism
Protocatechuate 3,4−dioxygenase beta subunit
Phosphatidylinositol kinase/protein kinase, PI−3 family
Pterin−4a−carbinolamine dehydratase
Membrane−bound metal−dependent hydrolase YbcI
Uncharacterized conserved protein YcaQ
PAS domain
Predicted lactoylglutathione lyase
Uncharacterized protein, vWA domain
Alcohol dehydrogenase, class IV
Transcriptional regulator MalT
ABC−type branched−chain amino acid transport system
Phosphohistidine phosphatase SixA
Predicted benzoate:H+ symporter BenE
Uncharacterized protein YjiK
Mg2+/citrate symporter
3−methyladenine DNA glycosylase AlkD
Ca2+/H+ antiporter
Uncharacterized conserved protein YndB
0.00
0.25
0.50
0.75
1.00
Proportion of genomes

Figure 3

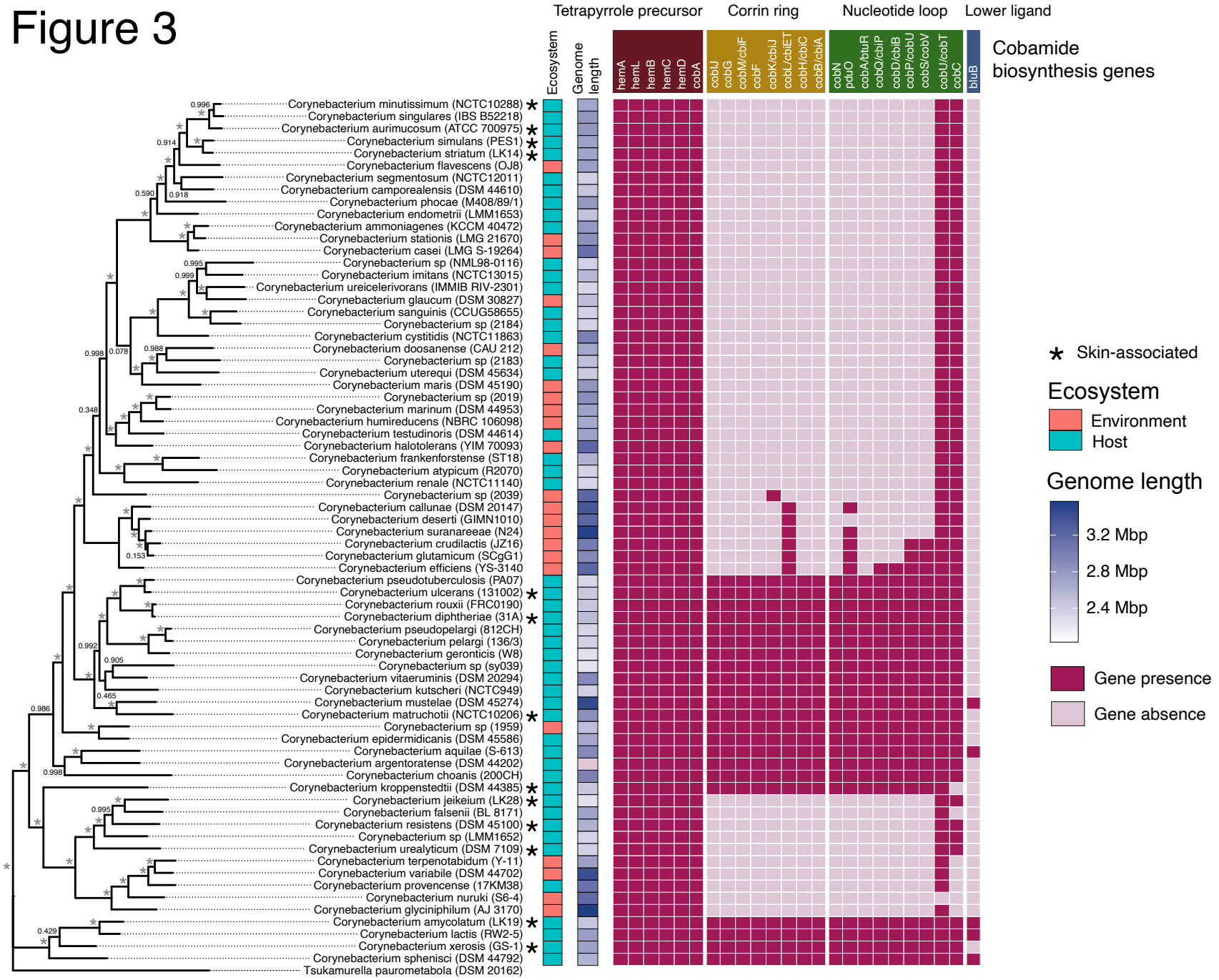
Tetrapyrrole precursor
Corrin ring
Nucleotide loop
Lower ligand
Ecosystem
Genome length
hemA
hemL
hemB
hemC
hemD
cobA
cobU
cobG
cobM/cbiF
cobF
cobK/cbiJ
cobL/cbiET
cobH/cbiC
cobB/cbiA
cobN
pduO
cobA/btuR
cobQ/cbiP
cobD/cbiB
cobP/cobU
cobS/cobV
cobU/cobT
cobC
bluB
Cobamide biosynthesis genes
Corynebacterium minutissimum (NCTC10288)
Corynebacterium singulares (IBS B52218)
Corynebacterium aurimucosum (ATCC 700975)
Corynebacterium simulans (PES1)
Corynebacterium striatum (LK14)
Corynebacterium flavescens (OJ8)
Corynebacterium segmentosum (NCTC12011)
Corynebacterium camporealensis (DSM 44610)
Corynebacterium phocae (M408/89/1)
Corynebacterium endometrii (LMM1653)
Corynebacterium ammoniagenes (KCCM 40472)
Corynebacterium stationis (LMG 21670)
Corynebacterium casei (LMG S-19264)
Corynebacterium sp (NML98-0116)
Corynebacterium imitans (NCTC13015)
Corynebacterium ureicelerivorans (IMMIB RIV-2301)
Corynebacterium glaucum (DSM 30827)
Corynebacterium sanguinis (CCUG58655)
Corynebacterium sp (2184)
Corynebacterium cystitidis (NCTC11863)
Corynebacterium doosanense (CAU 212)
Corynebacterium sp (2183)
Corynebacterium uterequi (DSM 45634)
Corynebacterium maris (DSM 45190)
Corynebacterium sp (2019)
Corynebacterium marinum (DSM 44953)
Corynebacterium humireducens (NBRC 106098)
Corynebacterium testudinoris (DSM 44614)
Corynebacterium halotolerans (YIM 70093)
Corynebacterium frankenforstense (ST18)
Corynebacterium atypicum (R2070)
Corynebacterium renale (NCTC11140)
Corynebacterium sp (2039)
Corynebacterium callunae (DSM 20147)
Corynebacterium deserti (GIMN1010)
Corynebacterium suranareeae (N24)
Corynebacterium crudilactis (JZ16)
Corynebacterium glutamicum (SCgG1)
Corynebacterium efficiens (YS-3140)
Corynebacterium pseudotuberculosis (PA07)
Corynebacterium ulcerans (131002)
Corynebacterium rouxii (FRC0190)
Corynebacterium diphtheriae (31A)
Corynebacterium pseudopelargi (812CH)
Corynebacterium pelargi (136/3)
Corynebacterium geronticis (W8)
Corynebacterium sp (sy039)
Corynebacterium vitaeruminis (DSM 20294)
Corynebacterium kutscheri (NCTC949)
Corynebacterium mustelae (DSM 45274)
Corynebacterium matruchotii (NCTC10206)
Corynebacterium sp (1959)
Corynebacterium epidermidicanis (DSM 45586)
Corynebacterium aquilae (S-613)
Corynebacterium argentoratense (DSM 44202)
Corynebacterium choanis (200CH)
Corynebacterium kroppenstedtii (DSM 44385)
Corynebacterium jeikeium (LK28)
Corynebacterium falsenii (BL 8171)
Corynebacterium resistens (DSM 45100)
Corynebacterium sp (LMM1652)
Corynebacterium urealyticum (DSM 7109)
Corynebacterium terpenotabidum (Y-11)
Corynebacterium variabile (DSM 44702)
Corynebacterium provencense (17KM38)
Corynebacterium nuruki (S6-4)
Corynebacterium glyciniphilum (AJ 3170)
Corynebacterium amycolatum (LK19)
Corynebacterium lactis (RW2-5)
Corynebacterium xerosis (GS-1)
Corynebacterium sphenisci (DSM 44792)
Tsukamurella paurometabola (DSM 20162)
Skin-associated
Ecosystem
Environment
Host
Genome length
3.2 Mbp
2.8 Mbp
2.4 Mbp
Gene presence
Gene absence

Figure 4

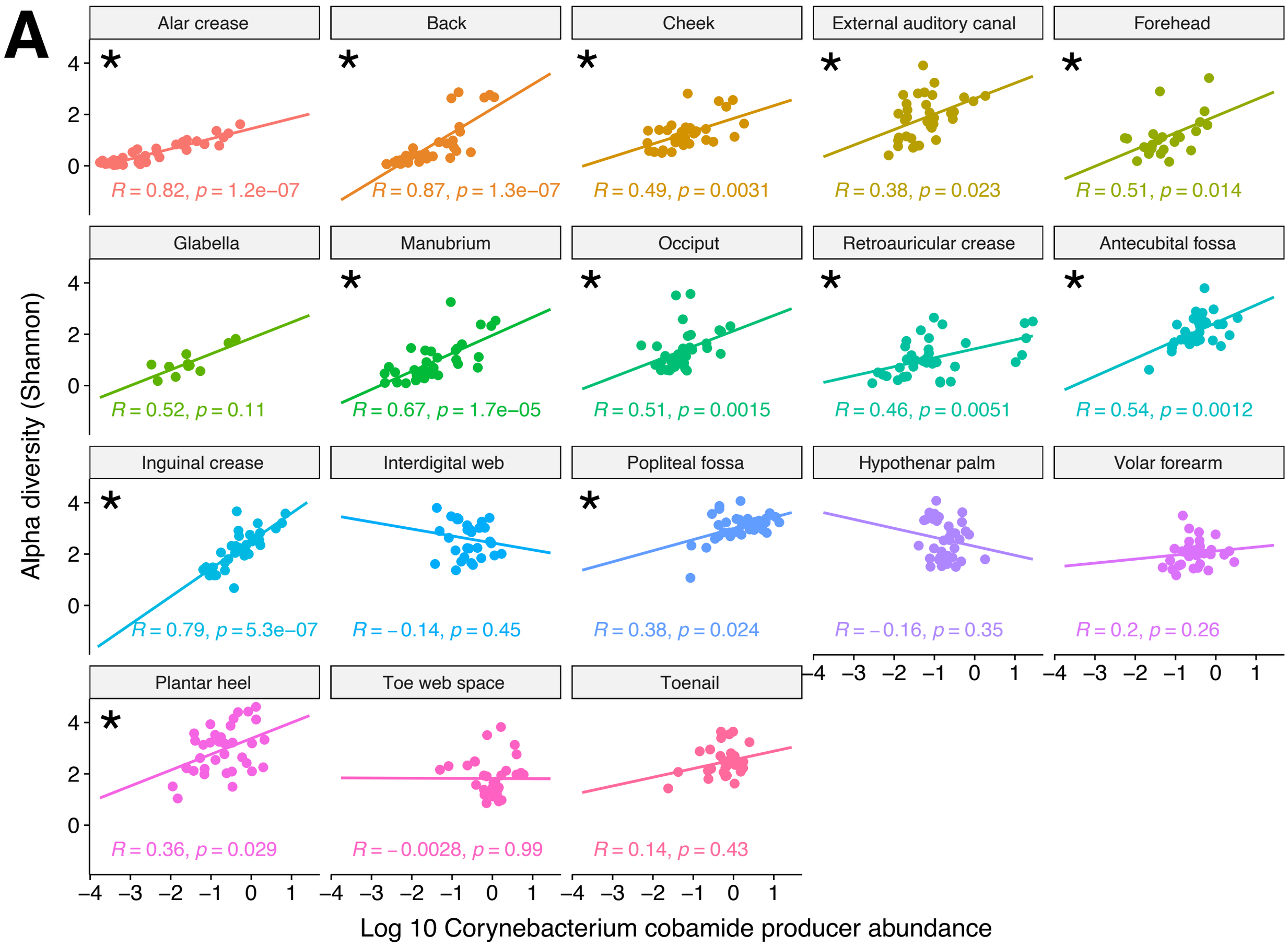
A
Alar crease
Back
Cheek
External auditory canal
Forehead
R = 0.82, p = 1.2e−07
R = 0.87, p = 1.3e−07
R = 0.49, p = 0.0031
R = 0.38, p = 0.023
R = 0.51, p = 0.014
Glabella
Manubrium
Occiput
Retroauricular crease
Antecubital fossa
R = 0.52, p = 0.11
R = 0.67, p = 1.7e−05
R = 0.51, p = 0.0015
R = 0.46, p = 0.0051
R = 0.54, p = 0.0012
Inguinal crease
Interdigital web
Popliteal fossa
Hypothenar palm
Volar forearm
R = 0.79, p = 5.3e−07
R = −0.14, p = 0.45
R = 0.38, p = 0.024
R = −0.16, p = 0.35
R = 0.2, p = 0.26
Plantar heel
Toe web space
Toenail
R = 0.36, p = 0.029
R = −0.0028, p = 0.99
R = 0.14, p = 0.43
Alpha diversity (Shannon)
Log 10 Corynebacterium cobamide producer abundance

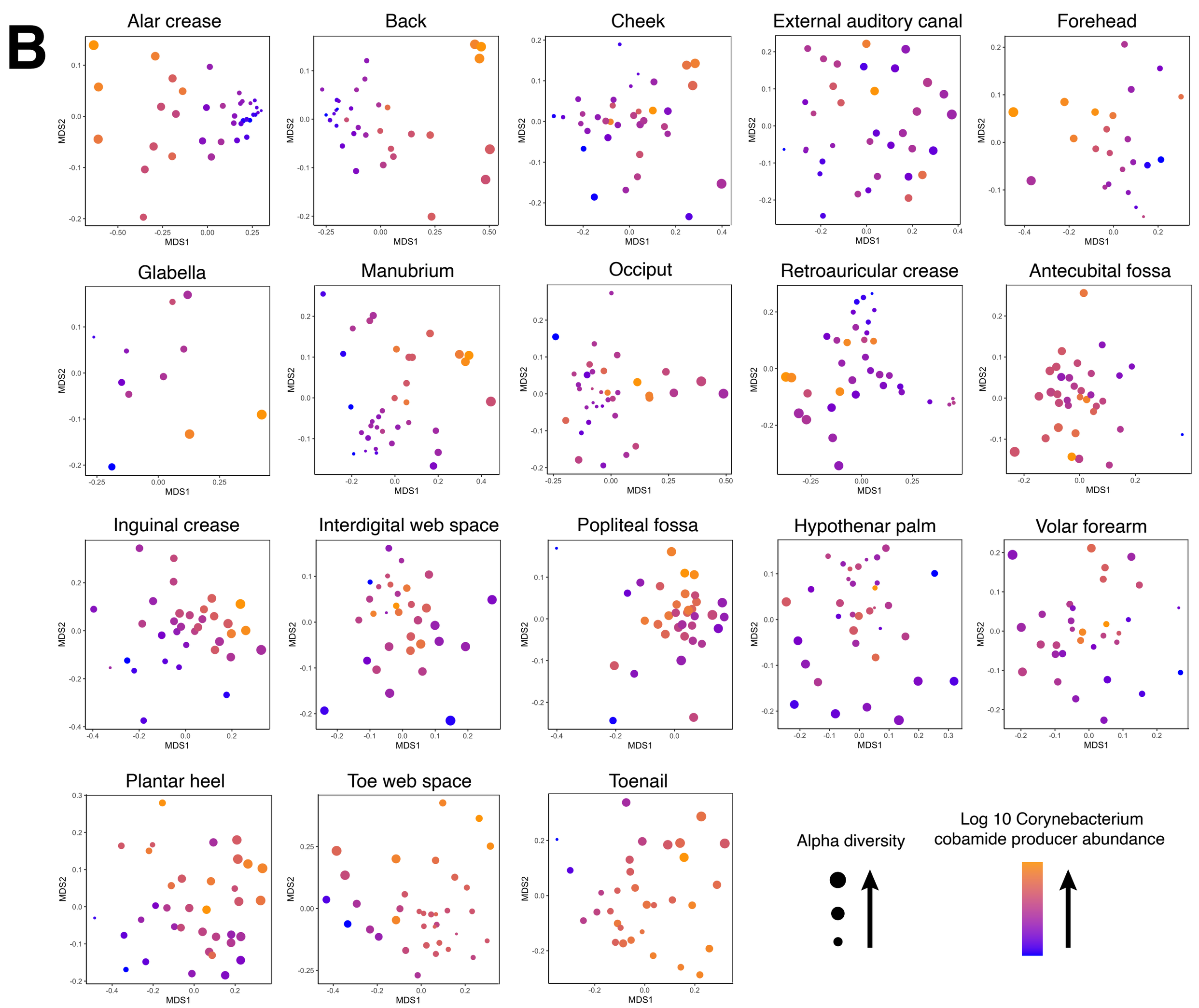
B
Alar crease
Back
Cheek
External auditory canal
Forehead
Glabella
Manubrium
Occiput
Retroauricular crease
Antecubital fossa
Inguinal crease
Interdigital web space
Popliteal fossa
Hypothenar palm
Volar forearm
Plantar heel
Toe web space
Toenail
MDS1
MDS2
Alpha diversity
Log 10 Corynebacterium cobamide producer abundance

Figure 5

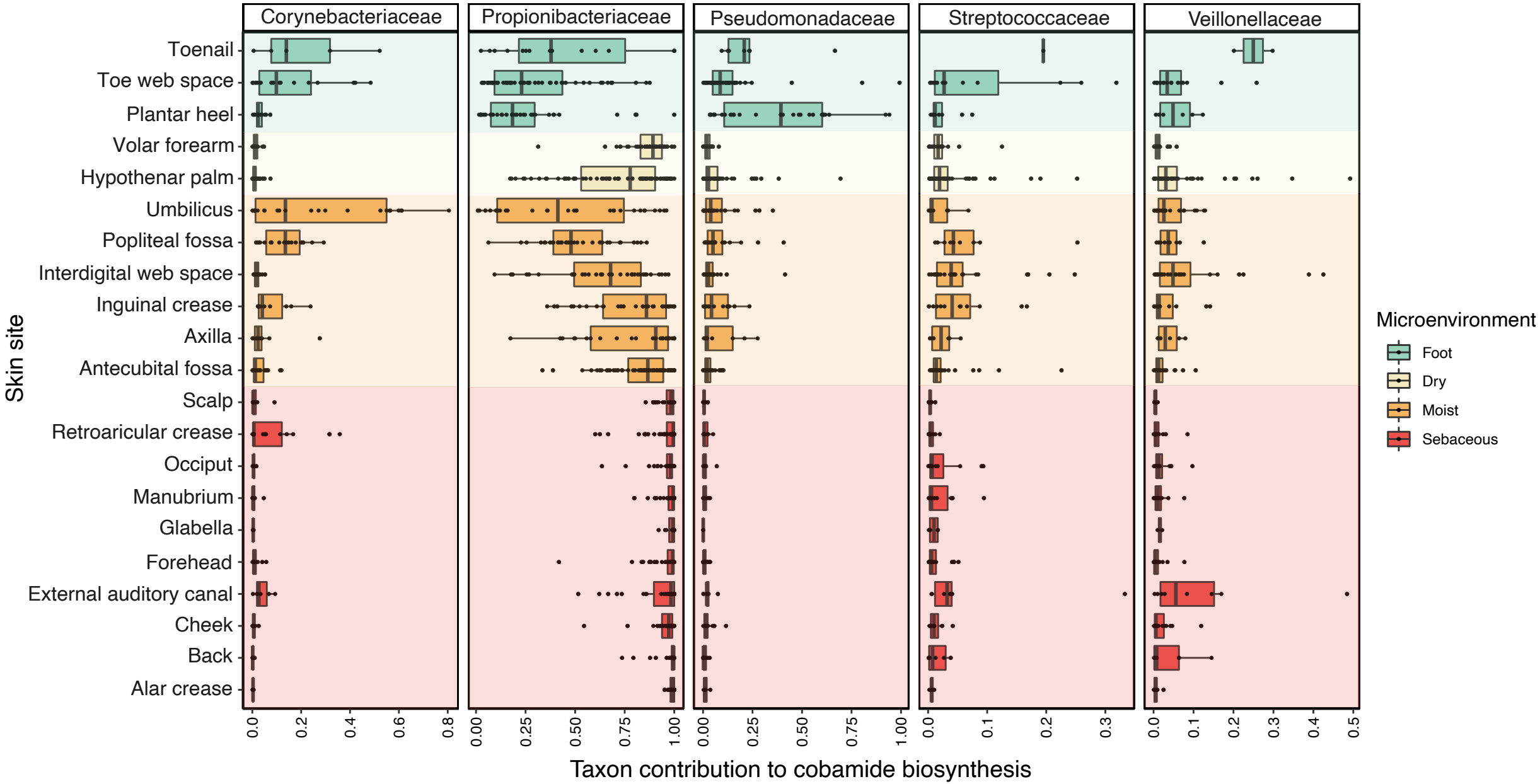
Corynebacteriaceae
Propionibacteriaceae
Pseudomonadaceae
Streptococcaceae
Veillonellaceae
Skin site
Toenail
Toe web space
Plantar heel
Volar forearm
Hypothenar palm
Umbilicus
Popliteal fossa
Interdigital web space
Inguinal crease
Axilla
Antecubital fossa
Scalp
Retroaricular crease
Occiput
Manubrium
Glabella
Forehead
External auditory canal
Cheek
Back
Alar crease
0.0
0.2
0.4
0.6
0.8
0.00
0.25
0.50
0.75
1.00
0.0
0.1
0.2
0.3
0.0
0.1
0.2
0.3
0.4
0.5
Taxon contribution to cobamide biosynthesis
Microenvironment
Foot
Dry
Moist
Sebaceous

Figure 6

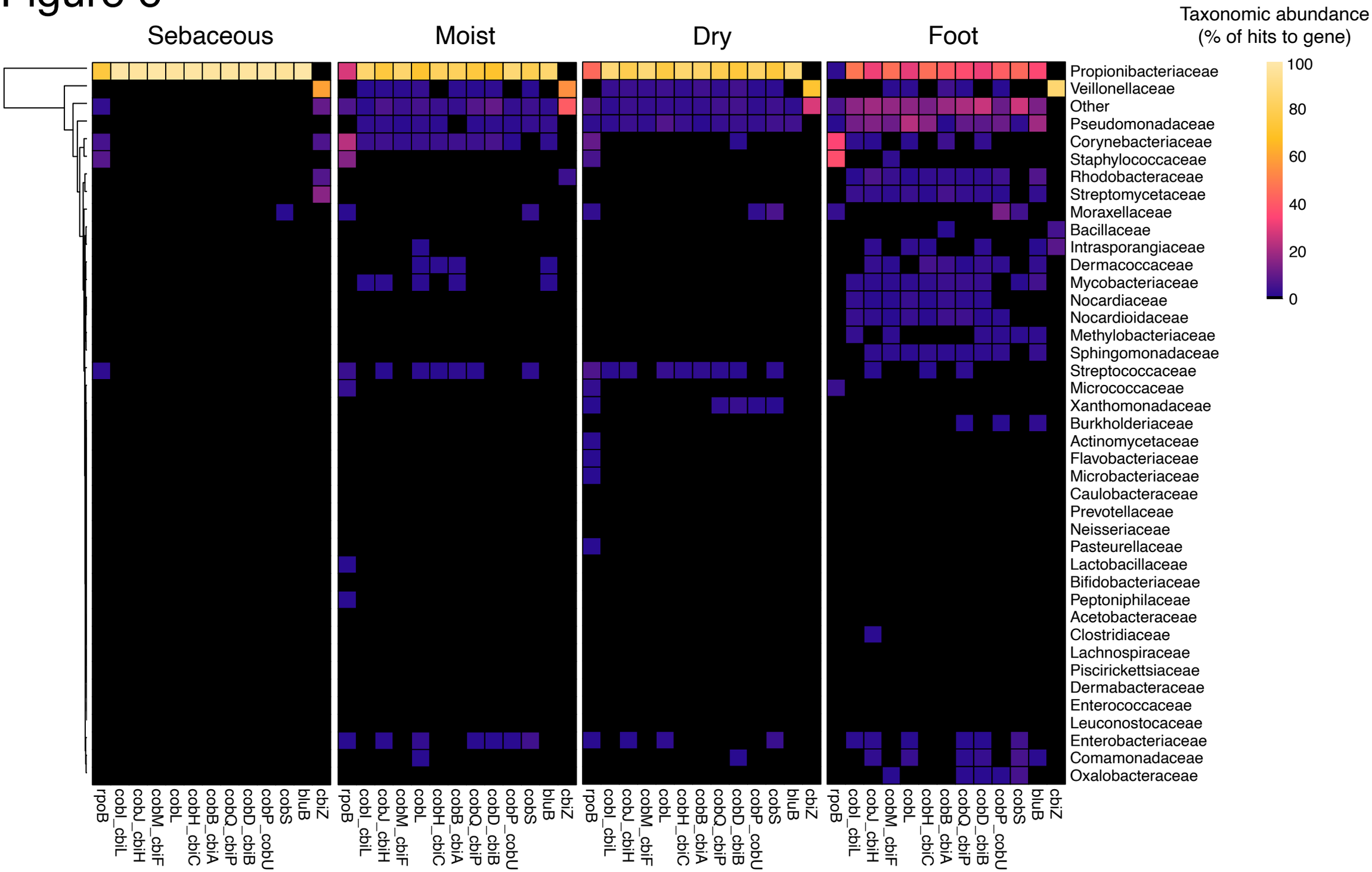
Sebaceous
Moist
Dry
Foot
Taxonomic abundance
(% of hits to gene)
100
80
60
40
20
0
Propionibacteriaceae
Veillonellaceae
Other
Pseudomonadaceae
Corynebacteriaceae
Staphylococcaceae
Rhodobacteraceae
Streptomycetaceae
Moraxellaceae
Bacillaceae
Intrasporangiaceae
Dermacoccaceae
Mycobacteriaceae
Nocardiaceae
Nocardioidaceae
Methylobacteriaceae
Sphingomonadaceae
Streptococcaceae
Micrococcaceae
Xanthomonadaceae
Burkholderiaceae
Actinomycetaceae
Flavobacteriaceae
Microbacteriaceae
Caulobacteraceae
Prevotellaceae
Neisseriaceae
Pasteurellaceae
Lactobacillaceae
Bifidobacteriaceae
Peptoniphilaceae
Acetobacteraceae
Clostridiaceae
Lachnospiraceae
Piscirickettsiaceae
Dermabacteraceae
Enterococcaceae
Leuconostocaceae
Enterobacteriaceae
Comamonadaceae
Oxalobacteraceae
rpoB
cobI_cbiL
cobJ_cbiH
cobM_cbiF
cobL
cobH_cbiC
cobB_cbiA
cobQ_cbiP
cobD_cbiB
cobP_cobU
cobS
bluB
cbiZ

Figure 7

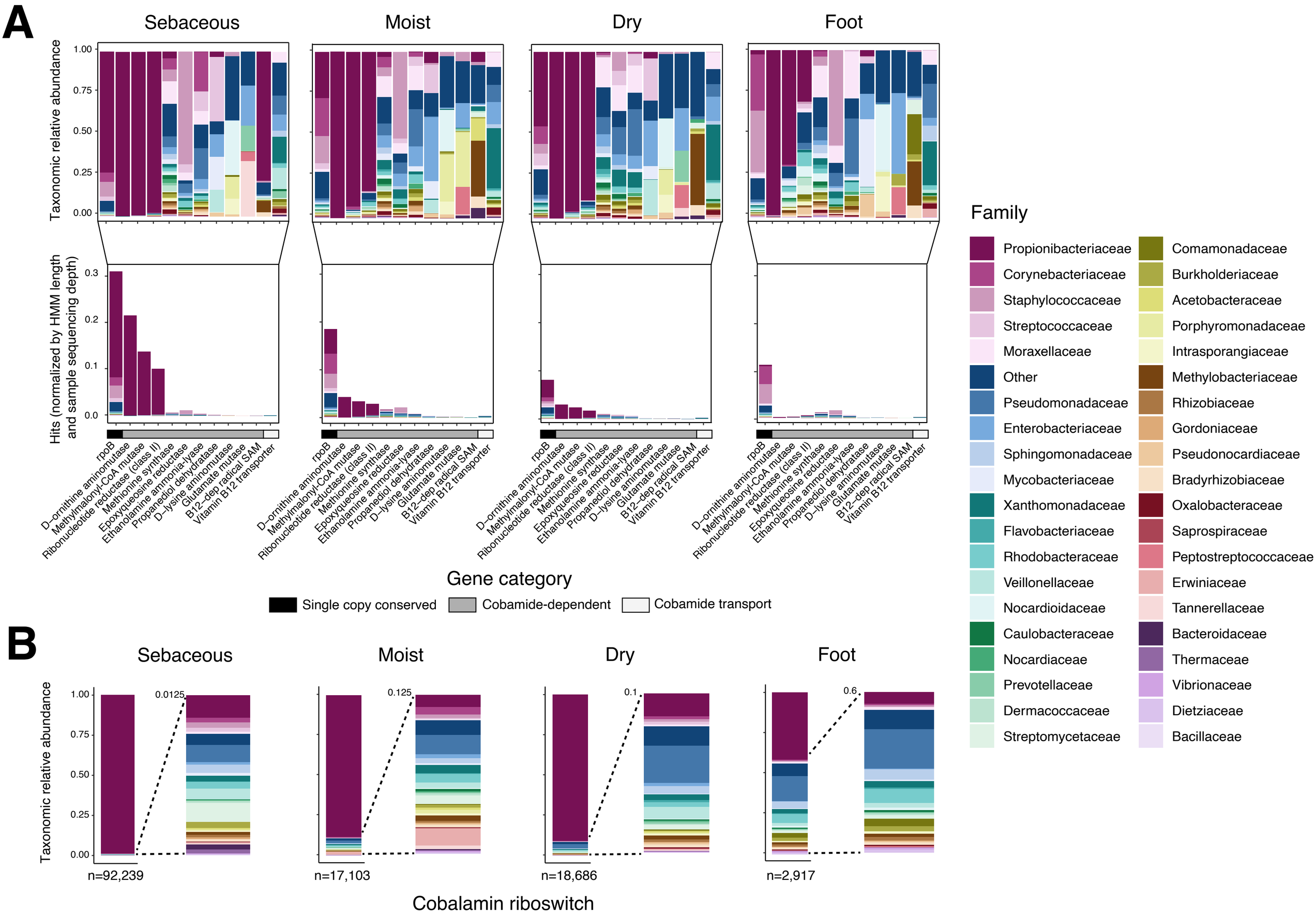
A
Sebaceous
Moist
Dry
Foot
Taxonomic relative abundance
1.00
0.75
0.50
0.25
0.00
Hits (normalized by HMM length and sample sequencing depth)
0.3
0.2
0.1
0.0
rpoB
D−ornithine aminomutase
Methylmalonyl−CoA mutase
Ribonucleotide reductase (class II)
Methionine synthase
Epoxyqueosine reductase
Ethanolamine ammonia−lyase
Propanediol dehydratase
D−lysine aminomutase
Glutamate mutase
B12−dep radical SAM
Vitamin B12 transporter
Gene category
Single copy conserved
Cobamide-dependent
Cobamide transport
Family
Propionibacteriaceae
Corynebacteriaceae
Staphylococcaceae
Streptococcaceae
Moraxellaceae
Other
Pseudomonadaceae
Enterobacteriaceae
Sphingomonadaceae
Mycobacteriaceae
Xanthomonadaceae
Flavobacteriaceae
Rhodobacteraceae
Veillonellaceae
Nocardioidaceae
Caulobacteraceae
Nocardiaceae
Prevotellaceae
Dermacoccaceae
Streptomycetaceae
Comamonadaceae
Burkholderiaceae
Acetobacteraceae
Porphyromonadaceae
Intrasporangiaceae
Methylobacteriaceae
Rhizobiaceae
Gordoniaceae
Pseudonocardiaceae
Bradyrhizobiaceae
Oxalobacteraceae
Saprospiraceae
Peptostreptococcaceae
Erwiniaceae
Tannerellaceae
Bacteroidaceae
Thermaceae
Vibrionaceae
Dietziaceae
Bacillaceae
B
Sebaceous
Moist
Dry
Foot
Taxonomic relative abundance
1.00
0.75
0.50
0.25
0.00
0.0125
0.125
0.1
0.6
n=92,239
n=17,103
n=18,686
n=2,917
Cobalamin riboswitch

Figure 8

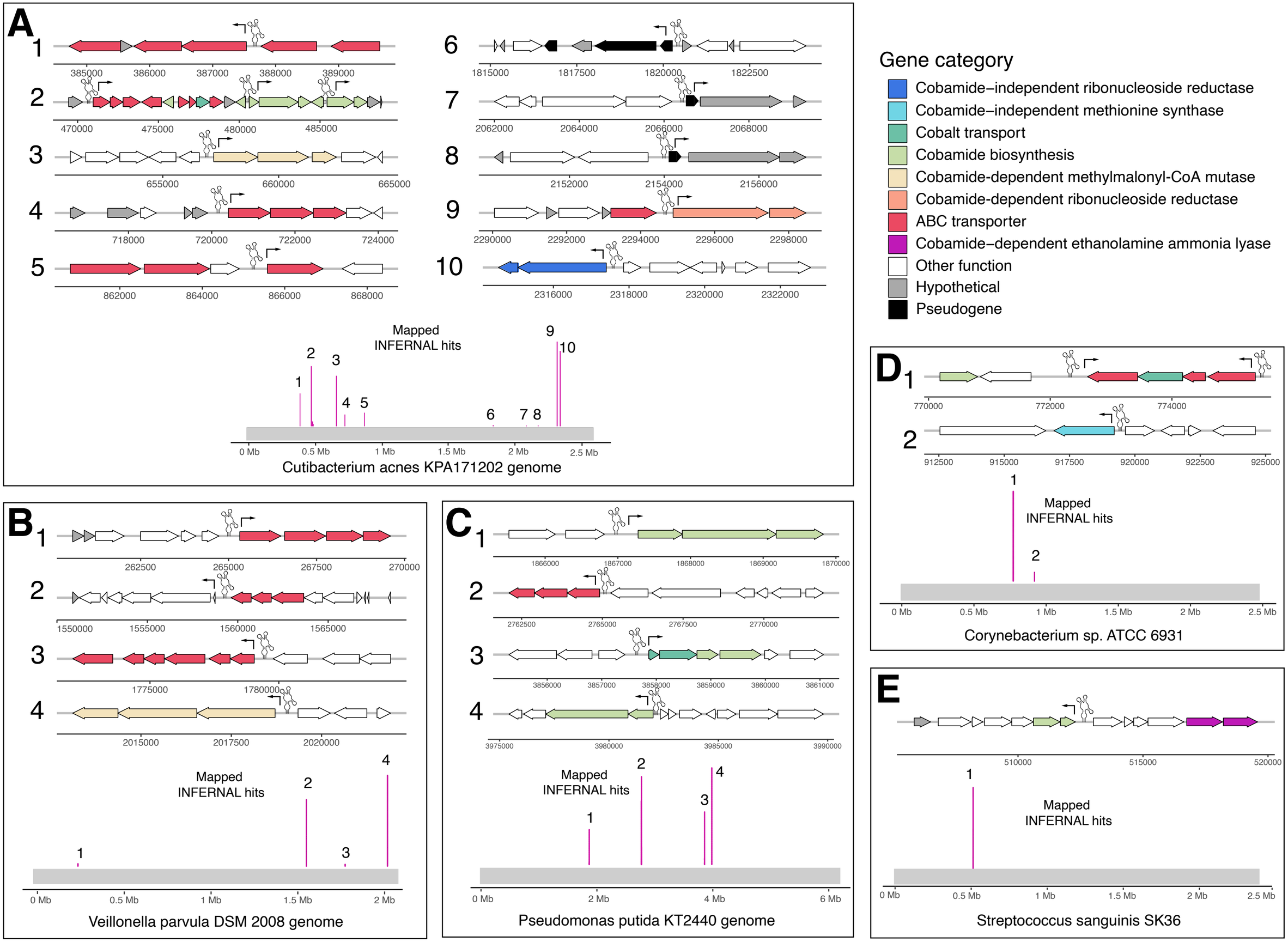
A
Mapped INFERNAL hits
Cutibacterium acnes KPA171202 genome
Gene category
Cobamide–independent ribonucleoside reductase
Cobamide–independent methionine synthase
Cobalt transport
Cobamide biosynthesis
Cobamide-dependent methylmalonyl-CoA mutase
Cobamide-dependent ribonucleoside reductase
ABC transporter
Cobamide–dependent ethanolamine ammonia lyase
Other function
Hypothetical
Pseudogene
B
Mapped INFERNAL hits
Veillonella parvula DSM 2008 genome
C
Mapped INFERNAL hits
Pseudomonas putida KT2440 genome
D
Mapped INFERNAL hits
Corynebacterium sp. ATCC 6931
E
Mapped INFERNAL hits
Streptococcus sanguinis SK36

Supplementary Figure 1

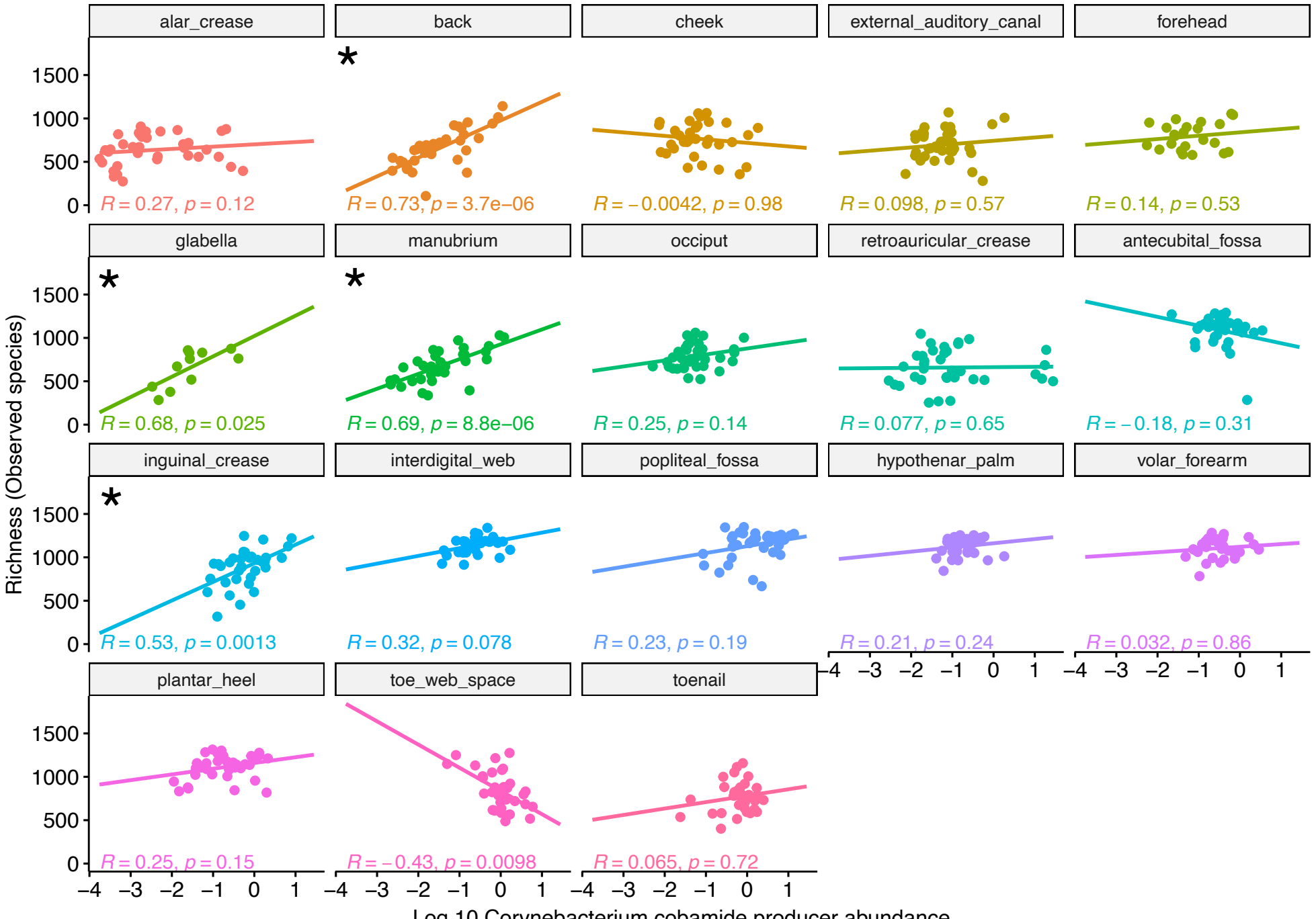

Supplementary Figure 2

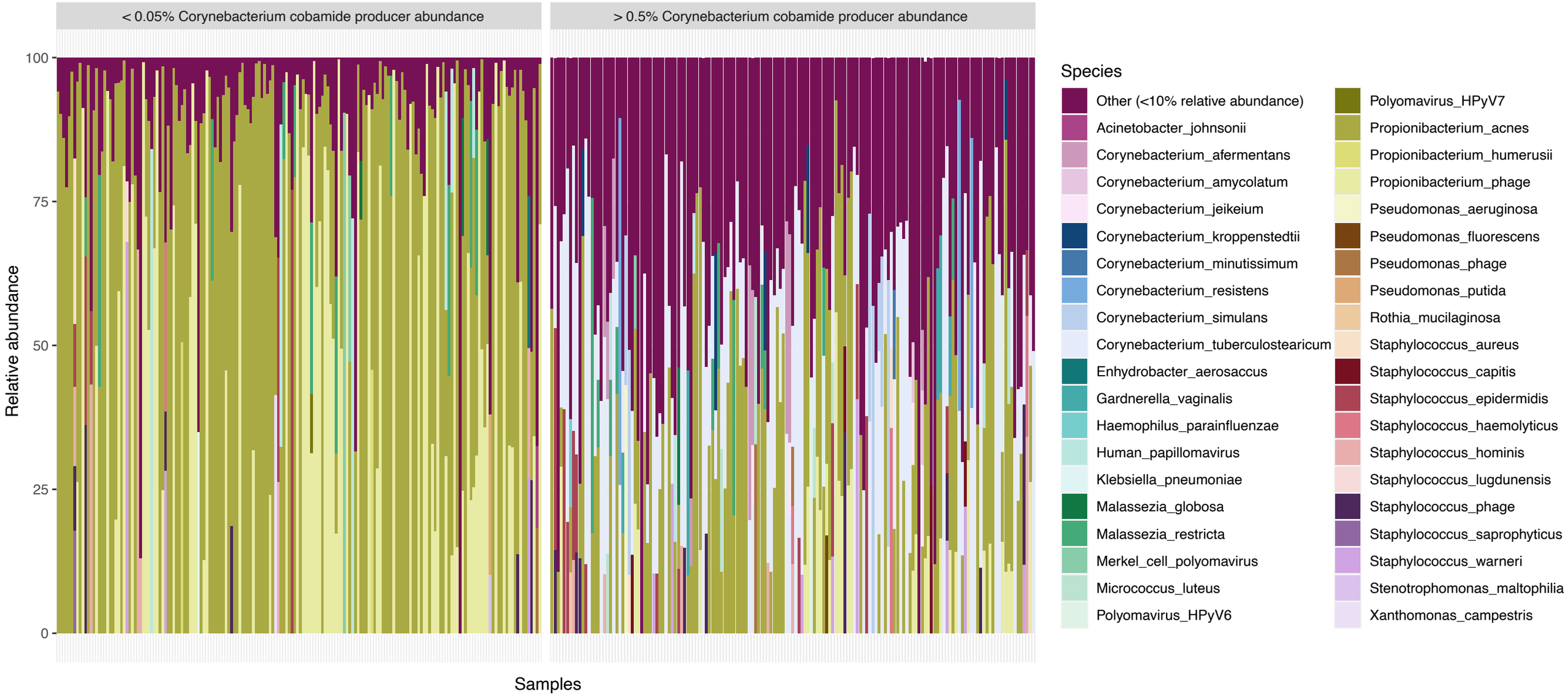
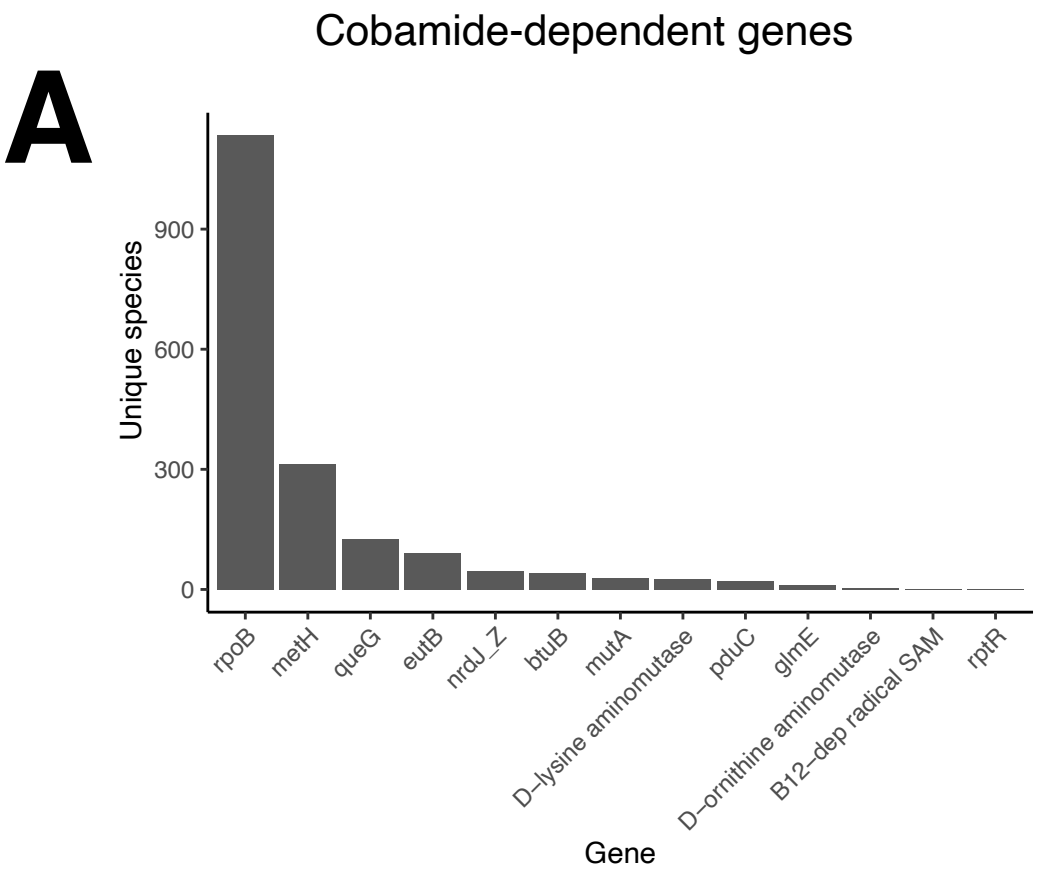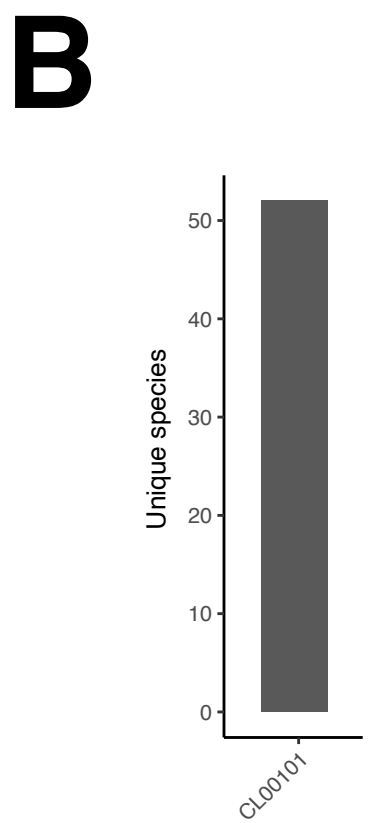
Supplementary Figure 3